

In Vivo Structural Neuroanatomy of Corpus Callosum in Alzheimer's Disease and Mild Cognitive Impairment Using Different MRI Techniques: A Review

Margherita Di Paola^{a,b,*}, Gianfranco Spalletta^a and Carlo Caltagirone^{a,c}

^a*Clinical and Behavioural Neurology, IRCCS Santa Lucia Foundation, Rome, Italy*

^b*Department of Internal Medicine and Public Health, University of L'Aquila, Italy*

^c*Department of Neurological Neuroscience, University of Rome "Tor Vergata", Italy*

Handling Associate Editor: Cindy Carlsson

Accepted 27 November 2009

Abstract. The corpus callosum (CC), which connects the two cerebral hemispheres, is the largest white matter fiber bundle in the human brain. This structure presents a peculiar myelination pattern: it has small diameter fibers, located in the genu, which myelinate much later in normal development, and large diameter fibers of the splenium, which myelinate early in development. Although the pathology of AD mainly involves the cerebral gray matter structure, there is evidence that white matter may also be involved. To illustrate callosal white matter changes in AD pathology, in this review we summarize *in vivo* imaging studies in humans, focusing on region of interest, voxel-based morphometry, diffusion-weighted imaging, and diffusion tensor imaging techniques. Our aims were to identify where in the CC, when in the different stages of AD, and how callosal changes can be detected with different MRI techniques. Results showed that changes in the anterior (genu and anterior body) as well as in the posterior (isthmus and splenium) portions of the CC might already be present in the early stages of AD. These findings support the hypothesis that two mechanisms, Wallerian degeneration and myelin breakdown, might be responsible for the region-specific changes detected in AD patients. Wallerian degeneration affects the posterior CC subregion, which receives axons directly from those brain areas (temporo-parietal lobe regions) primarily affected by the AD pathology. Instead, the myelin breakdown process affects the later-myelinating CC subregion and explains the earlier involvement of the genu in CC atrophy.

Keywords: Alzheimer's disease, corpus callosum, diffuse tensor imaging, diffusion-weighted imaging, mild cognitive impairment, region of interest, voxel-based morphometry

INTRODUCTION

Although research in the field of Alzheimer's disease (AD) has basically focused on gray matter (GM) de-

generation, a number of investigations have also documented a general white matter (WM) pathology associated with AD [1–6]. The corpus callosum (CC) has been implicated in this process [7–21]. In particular, it has been suggested that callosal atrophy in AD is the anatomical correlate of Wallerian degeneration of commissural nerve fibers. Thus, it might occur as a consequence of the death of projecting pyramidal cells in layer III of the neocortex and might reflect the pat-

*Correspondence to: Dr. Margherita Di Paola, IRCCS Santa Lucia Foundation, Via Ardeatina 306, 00179 Rome, Italy. Tel.: +39 06 51501215; Fax: +39 06 51501213; E-mail: m.dipaola@hsantalucia.it.

tern of neocortical neurodegeneration and the resulting cognitive dysfunction [13,22–26].

Unfortunately, in spite of the plethora of studies on callosal changes in AD, results are unclear. Although it is commonly accepted that in AD patients, CC atrophy is mainly located in the anterior (genu and anterior body) and posterior (isthmus and splenium) subregions, it is less clear whether this finding is consistent in the different stages of AD pathology and across different methods.

In fact, the main result mentioned above, that is atrophy mainly in the callosal anterior and posterior subregions, comes from studies of AD groups that included patients in different illness stages, ranging from mild to severe dementia [7,8,10–12,14–19,23–25,27–43] and sometimes selected using different diagnostic criteria [10,14].

Furthermore, it has been found that different methods can produce different results. With regard to the region of interest (ROI) studies, for example, it has been shown that the earlier findings relied on manually tracing the CC and on the common callosal parcellation schemes (i.e., according to Witelson [19,44]; Weis [45–47]; or Hampel [11,18]) have generated a controversy regarding the assumed topography of callosal fibers [48]. In fact, in a previous study, we demonstrated that pre-defining callosal regions can give rise to misleading results [7]. This is also true for the voxel-based morphometry (VBM) technique. Senjem and colleagues [49] found that changes in the image processing chain of VBM noticeably influenced the results of inter-group morphometric comparisons. For example, the so-called “Optimized VBM” produced different results from those obtained with standard VBM.

Diffuse tensor imaging (DTI) studies have also produced different results. The vast majority of DTI studies are calculated as the diffusion parameters mean diffusivity (MD), which is a measure of the average motion of water molecules, independent of tissue directionality, and fractional anisotropy (FA), which measures the directionality of water diffusion. The pathological process of AD should alter both MD and FA values in the direction of lesser restriction on the movement of water and, therefore, with an increase in diffusivity (MD) and a decrease in anisotropy (FA). Nevertheless, in anatomically well-oriented structures, such as the CC, these two parameters seem to remain in the normal range. Thus, many DTI studies conclude that in the CC there is no difference between AD patients and healthy controls (HC).

Two main open questions motivated the present review: i) how early callosal atrophy occurs in AD and

whether the callosal changes involving the anterior and the posterior subregions can already be detected in mild AD and amnesic mild cognitive impairment (MCI); and ii) which magnetic resonance imaging (MRI) techniques are most useful for detecting callosal changes. Therefore, this review is focused on exploring how the CC changes in the different stages of AD and in MCI (i.e., in the preclinical stage of dementia and in the group at highest risk for developing dementia) [50–52], and which measurements have been applied to study these modifications *in vivo*.

MATERIAL AND METHODS

A detailed search of the literature was conducted. For our purposes, the database was selected using PubMed Services to research the following keywords: corpus callosum, white matter, Alzheimer’s disease, mild cognitive impairment, region of interest, voxel-based morphometry, diffusion-weighted imaging, and diffusion tensor imaging. In examining research results, we paid attention to the clinical features of the patient groups to classify results obtained evaluating heterogeneous groups of patients (i.e., AD and/or MCI patients with illness severity) separately from those obtained studying homogeneous groups of patients (i.e., only mild AD or only amnesic MCI). This was done to keep separate data in which the presence of more severe patients (e.g., severe AD) could bias results and to investigate whether a specific pattern of callosal degeneration was associated with different illness stages (from amnesic MCI to mild, moderate and severe AD). Thus, using the MRI modality as a starting point, we reviewed an extensive body of literature focusing mainly on structural neuroimaging (i.e., ROI and VBM) and quantitative parametric mapping (i.e., diffusion-weighted imaging (DWI) and DTI).

Initially, 52 studies were selected as potential candidates for review. Studies were included if they: 1) were brain structural MRI studies published from January 1997 to March 2009; 2) compared AD or MCI patients with a HC group; and 3) were published in the English language. We also hand-searched relevant journals and inspected the bibliographies of all major articles to find other relevant publications. Historically important and conceptually related articles were included as well. One study was excluded from the review [53] because it did not compare AD patients with a HC group. Concerning the nomenclature of the CC subregions, to be consistent across studies we refer to

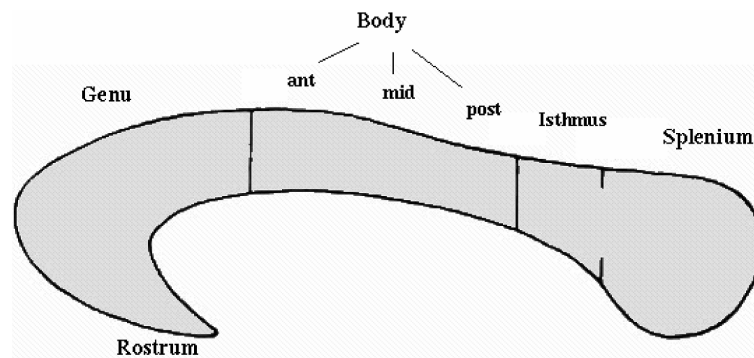


Fig. 1. Schematic view of corpus callosum for nomenclature. The image shows the different subregions of the CC regardless of splitting method and callosal fiber topography.

the different subregions of the CC as follows: rostrum, genu, body (split into anterior, mid, and posterior), isthmus, and splenium (see Fig. 1 for a schematic view).

REGION OF INTEREST STUDIES

Early morphometric MRI studies of the CC in AD quantified atrophic changes using ROI analysis. In general, to perform a ROI analysis a high spatial resolution 3D brain sequence has to be acquired with an isotropic voxel (e.g., $1 \times 1 \times 1 \text{ mm}^3$), so that all three orthogonal planes can be inspected. This procedure also facilitates identification of anatomical landmarks for selection of the ROI. To obtain a better identification of the CC ROI, each MRI brain volume is usually positioned along the anterior-posterior commissure line. This is particularly important for obtaining a reliable measure of the CC, because it is sampled from its most medial part on a 1mm thick slice. Each ROI is identified by its landmarks and manually mapped. Then the voxels belonging to the ROI are colored to show the volume of the CC in mm^3 . According to the model used, an automatic procedure is applied to split the CC. To determine the size of the CC, several methodologies have been proposed for measuring its midsagittal surface area and regional divisions. In Fig. 2, we report the most frequently used methods. Finally, to reduce inter-individual variability in gross brain size, different reference measures, such as forebrain volume, cranial capacity, cross-sectional cerebral area, or normalization of the MRI brain volumes into the Talairach proportional stereotaxic space, are used either as a ratio [54,55] or as a covariate in the statistical model [56, 57]. In this way, gross brain size differences are ruled out.

ROI analysis is considered a robust, well-validated technique. However, it requires operator skills to define the boundaries of the structures to be investigated. Furthermore, it is time consuming, because the researcher has to draw the ROI manually, and allows studying only a limited number of anatomical regions chosen *a priori*.

Numerous ROI studies have investigated callosal changes in AD patients [7,10–12,14–19,24,25,27,28, 31,38,42,43]. Overall, these studies report a reduction of the total callosal area, specifically of the rostrum, genu, anterior body, isthmus, and splenium of the CC. It should be noted that the vast majority of these studies included AD patients with illness stages, ranging from mild to severe dementia (hereafter called AD “all stages”). Only a few studies investigated patients with fewer heterogeneous clinical features, such as those affected by mild or moderate AD, and they reported discrepant results. More specifically, while some studies on mild AD found atrophy in the posterior callosal subregions (isthmus and splenium) [9,11,13,19], others found no atrophy in callosal regions [45,58]. As far as we know, there is only one study [59] on moderate AD patients that describes a reduction of the anterior body, mid body, and isthmus in AD patients compared with HC. Likewise, inconsistent results have been reported in studies on subjects with MCI. In a study on amnesic MCI, Wang and colleagues [9] found atrophy in posterior subregions (isthmus and splenium). Yet, another research group [46] found no callosal changes when patients with amnesic MCI were compared with HC. By contrast, Thomann and coworkers [10] reported a reduction in the anterior subregion (rostrum, genu, anterior body) of the CC in a group of MCI patients with different cognitive subtypes (amnesic and multi-domain amnesic, hereafter called MCI “all subtypes”) using the ROI approach. Finally, Hallam et al. [43] re-

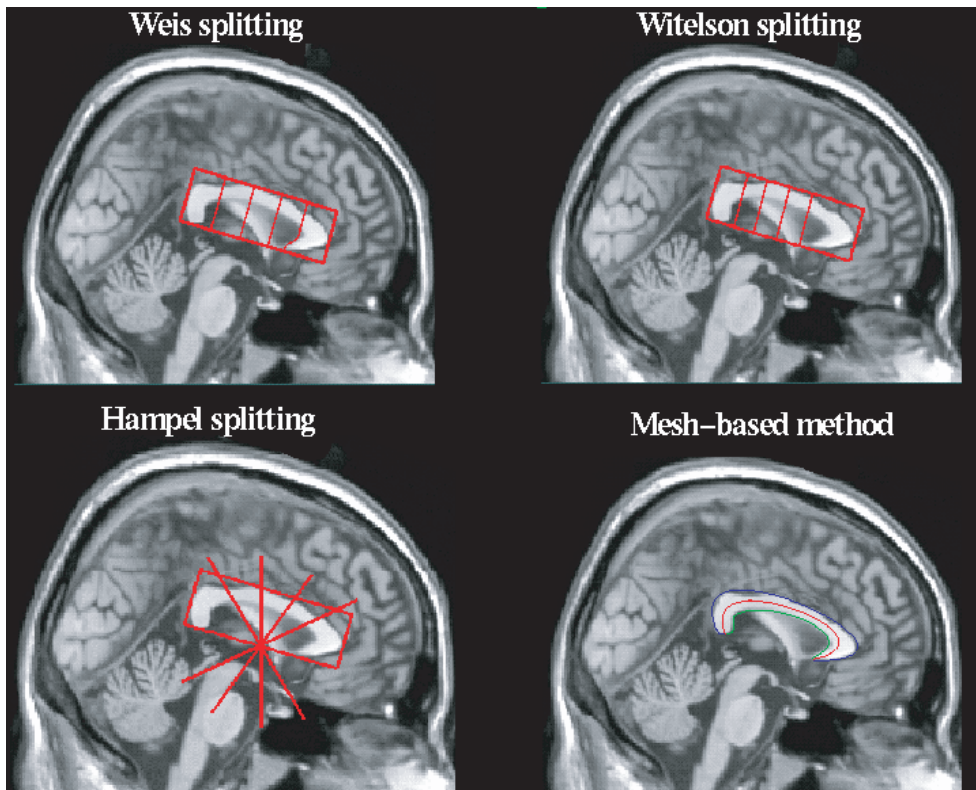


Fig. 2. Different corpus callosum manual tracing. In Weis splitting, the midsagittal slice of the CC is split into five distinct sectors of equal size along a line joining the most anterior and posterior points of the genu and splenium, respectively. Subregions are the following: CC1 = rostrum and genu, CC2 = rostral body, CC3 = midbody, CC4 = isthmus, CC5 = splenium. In Witelson splitting, the midsagittal slice of the CC is split into five distinct sectors of different percentages: 33%, 17%, 17%, 13%, 20% respectively. The subregions are: CC1 = rostrum, genu and anterior body, CC2 = midbody, CC3 = caudal body, CC4 = isthmus, CC5 = splenium. In Hampel splitting, the midsagittal slice of CC is split into five distinct sectors of equal percentage (36%) along a line joining the most anterior and posterior points of genu and splenium respectively. The subregions are: CC1 = rostrum, CC2 = anterior truncus, CC3 = middle truncus, CC4 = posterior truncus, CC5 = splenium. In the Mesh-based method, there is no splitting. Upper and lower callosal boundaries are manually outlined in the midsagittal section. Then, the spatial average from 100 equidistant surface points representing the upper and lower boundaries is calculated. The result is a new midline segment (the spatial average), also consisting of 100 equidistant points. Finally, the midline segment is quantified, so that it corresponds to CC thickness.

ported no difference between a mild ambiguous group (i.e., with a cognitive profile similar to that of multi-domain MCI) and HC.

Recently, our group [21] applied a well-validated structural analysis technique, that is, the computational mesh-based method, to map callosal thickness [60–63] and to study the CC changes in three distinct homogeneous groups of patients with mild AD, severe AD, and amnesic MCI compared with HC. The main finding of our study was reduced thickness in the callosal genu, anterior body, and splenium in severe AD patients compared with HC. The callosal reductions in the milder and pre-clinical stages of AD appeared to be less pronounced (i.e., they were more restricted spatially). When mild AD patients were compared with HC, we observed reduced callosal thickness within the

callosal anterior third, as well as at the border between the anterior third and the anterior body. When amnesic MCI patients were compared with HC, reduced callosal thickness was found in the callosal posterior body and within the splenium near the callosal posterior end. Nevertheless, group differences between mild AD and amnesic MCI subjects and healthy controls were not confirmed by permutation testing (see Table 1 for technical details of the study).

VOXEL-BASED MORPHOMETRY STUDIES

After the ROI studies, a new imaging technique, VBM, was adopted to examine CC changes [64]. VBM is increasingly used to investigate differences in brain

morphology among groups. Indeed, it provides an estimate of inter-group differences in GM and WM density and/or volume on a voxelwise basis in a standardized space. The VBM protocol has been somewhat changed in the last few years to improve the preprocessing steps. In its previous version, called the “Optimized VBM” protocol, running in the framework of Statistical Parametric Mapping (SPM99, SPM2, Wellcome Department of Imaging Neuroscience, University College London, London, UK), a customized GM template is created and subsequently used to normalize all structural images to the stereotaxic MNI space. To create the customized GM template, all images (patients and controls) are first spatially normalized (12-parameter affine and $6 \times 8 \times 5$ basis functions) using the standard MNI template in SPM99 or SPM2. Then each normalized image is segmented into GM, WM, and cerebrospinal fluid (CSF). The normalized and segmented GM images are smoothed (isotropic kernel, usually with a FWHM between 8 and 12 mm) and averaged to create the customized GM template. Then all the original MR images in native space are segmented into GM, WM and CSF. The GM and the WM images are normalized to the customized GM template and the deformation parameters obtained from this are applied to all original images. This provides optimally normalized whole-brain images, which are segmented again into GM, WM, and CSF. Finally, all GM and WM images are modulated or not (to assess the absolute amount or concentration of a region of tissue [34] and smoothed with an FWHM kernel (the smoothing conforms the data more closely to the Gaussian field model underlying the statistical procedures used for making inferences about regionally specific effects). Smoothing also has the effect of rendering the data more normally distributed (by the central limit theorem). The intensity of the smoothed data in each voxel is a locally weighted average of GM density from a region of surrounding voxels; the size of the region is defined by the size of the smoothing kernel [64].

Although the current procedure is somewhat different from the original one, the logic of image preprocessing is the same. Briefly, in the unified segmentation step [65], implemented in the framework of Statistical Parametric Mapping (SPM5, Wellcome Department of Imaging Neuroscience, University College London, London, UK), images are normalized and segmented into GM and WM partitions and into CSF. For each subject, normalized segmented GM and WM are modulated or not and smoothed with a Gaussian Kernel (FWHM). In Fig. 3, we show a flow chart of Optimized VBM image processing.

Compared with ROI analysis, VBM analysis has the advantage of being a spatially specific and unbiased method for analyzing MR images. It is completely operator independent and provides a quantitative measure of the regional GM and WM volume or density at a voxel scale throughout the whole brain without choosing any *a priori* ROI [34,64].

The first VBM study on WM in moderate AD [66] reported the presence of diffuse atrophy within the CC but did not mention its specific location. Later works on AD “all stages” groups (more precisely on mild to moderate patients) reported conflicting results. Thomann et al. [10] found a significant loss of callosal volume in the anterior portion of the CC (rostrum, genu, and anterior body). Chaim and colleagues [8] reported a reduction in almost all subregions of the CC (genu, anterior and posterior body, isthmus, splenium), but mainly in the left hemisphere. Li et al. [42] found a reduction limited to the posterior CC subregions (isthmus and splenium), and, in agreement with Chaim et al. [8], prevalently on the left side of the CC.

We found only one VBM study [10] on callosal changes in MCI. However, it did not report differences in the CC in MCI subjects compared with HC.

In our study [20], we applied the VBM technique to study CC changes in patients with mild AD, severe AD, and amnesic MCI. We found atrophy in severe AD, specifically in the genu, anterior body, and splenium of the CC. Patients with mild AD presented a reduction in both the anterior and posterior CC, and those with amnesic MCI only in the anterior CC. Nevertheless, the results obtained on patients with mild AD and amnesic MCI were not supported by statistical correction for multiple comparisons. Recently, however, we replicated the study on a larger sample of patients with mild AD and amnesic MCI [21] and found a significant WM density reduction in the genu and splenium of the CC in patients with mild AD. In patients with amnesic MCI compared with HC, we found a reduction only in the genu of the CC (see Table 2 for technical details of the study).

DIFFUSION-WEIGHTED IMAGING AND DIFFUSION TENSOR IMAGING STUDIES

Diffusion imaging is a non-invasive MR technique adopted to study aspects of WM anatomy. It uses local water diffusion in the tissues as the starting point. Although the determinants of water diffusion in WM tissues are still not completely understood, there is

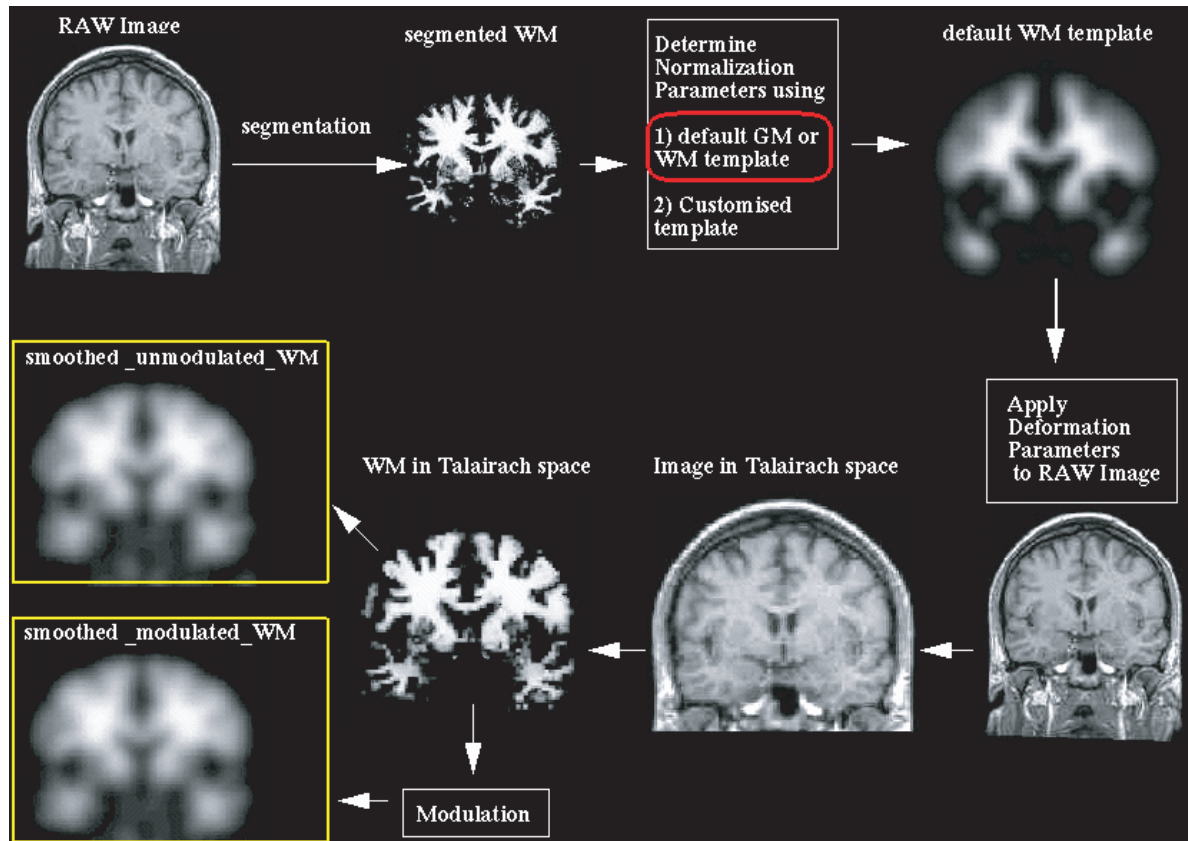


Fig. 3. Optimized Voxel-based Morphometry pipeline. Image shows the spatial processing steps of optimized VBM and the two resulting analyses. Templates used for normalization (gray matter or white matter) are indicated in red and the two analyses are indicated in yellow. Both affine and nonlinear basis function normalization are used in the technique.

general agreement that the physicochemical properties of the tissue (e.g., viscosity and temperature) as well as its structural components (macromolecules, membranes, and intracellular organelles) can substantially affect water diffusivity. In other words, diffusivity of water depends primarily on the presence of microscopic structural barriers in tissues that can alter the random motion of water molecules. Membranes of cell bodies, axons, and myelin sheaths randomly impede the movement of water in the brain tissue, facilitating diffusion of water molecules preferentially along their main direction. Such preferentially oriented diffusion is called anisotropic diffusion. DWI is a one-dimensional technique, that is, it is used to measure the projection of all molecular displacements along one direction at a time. Therefore, it is sufficient to apply diffusion gradients along only one direction. As DTI is a three-dimensional technique, diffusion gradients must be applied along at least six noncollinear, non-coplanar directions in order to obtain enough information to estimate the six independent elements of the diffusion tensor (D) (in [67]).

In general, apparent diffusion coefficient (ADC), MD, and FA have been used as the main diffusivity parameters. Although ADC measures the magnitude of water diffusion, it only provides a measure of the displacement of molecules in one direction; MD is a measure of the average motion of water molecules, independent of tissue directionality; and FA measures the directionality of water diffusion.

ADC, MD, and FA may be altered by changes caused by the pathological process of AD. Pathological disruption of cell membranes and loss of myelin and axonal processes should lessen the restrictions on water movement. Therefore, the diffusivity measured with ADC or with MD should increase. Furthermore, the loss of tissue organization should also cause a decrease in anisotropy (FA). It is assumed that reduced water diffusion parallel to axonal tracts or FA is indicative of axonal degeneration and that increased water diffusion perpendicular to axonal tracts or MD is associated with changes in water content, disruption, and partial break-

Table 1
ROI studies of CC

Study (year)	Sample	MMSE mean \pm SD (range)	MRI acquisition	ROI method	Positive findings	Negative findings
Kaufner et al. (1997)	-17 AD	17.3 \pm 6.4 (2-27)	1.5 T magnet. A T1-weighted volumetric scan (slice thickness = 5 mm)	Radial splitting in 4 subregions: the two anterior sectors (CC-1), three anterior body sectors (CC-2), three posterior body sectors (CC-3), and the two posterior sectors (CC-4)	Regional decreases of CC in AD patients compared with HC were most prominent in CC-1.	There were no significant differences in total CC area in AD patients compared with HC.
	-16 FTD	n.r.				
	-12 HC	29.4 \pm 0.9 (27-30)			Regional decreases were seen to a lesser extent in the two middle CC regions (CC-2 and CC-3).	
Lyo et al. (1997)	-162 AD:	16.1 \pm 6.4 (n.a.);	1.5 T magnet. A T1-weighted volumetric scan (slice thickness = 5 mm)	Witelson splitting	All regional areas of CC were smaller in all AD patients compared with HC.	
	n 49 AD	n.a. \pm n.a. (\geq 21)			Atrophy only in the posterior body, isthmus and splenium of CC in a subgroup of mild AD (n 49 MMSE \geq 21).	
	n 47 AD	n.a. \pm n.a. (20-16)				
	n 33 AD	n.a. \pm n.a. (15-11)				
	n 33 AD	n.a. \pm n.a. (\leq 10)				
	-28 MID	n.r.				
	-36 HC	28.9 \pm 1.3 (n.a.)				
Black et al. (2000)	-23 AD	18.1 \pm 5.4 (n.a.)	1.5 T magnet. A T1-weighted volumetric scan (slice thickness = 1.2 mm)	Witelson splitting	Reduction of total callosal area in AD patients compared with HC.	
	-17 HC	28.2 \pm 1.8 (n.a.)			Reduction of CC1 (genu) CC3 (anterior body) CC4 (posterior body) and CC5 (splenium) in AD patients compared with HC.	
Tomaiuolo et al. (2007)	-17 AD	n.a. \pm n.a. ($<$ 24)	1.5 T magnet. A T1-weighted volumetric scan (slice thickness = 1 \times 1 mm)	Witelson splitting	Reduction of total callosal area in AD patients compared with HC.	
	-17 HC	n.a. \pm n.a. ($>$ 28)			Reduction in rostrum, genu, anterior body, isthmus and splenium of CC in AD patients compared with HC.	
Hampel et al. (1998)	-14 AD:	11.4 \pm 8.6 (n.a.);	Two MRI sequences: -0.5 T magnet. A T1-weighted volumetric scan (slice thickness = 2.5 mm)	Hampel splitting	Absolute mean total callosal area was smaller in AD patients compared with HC.	
	n 4 AD mild	n.a. \pm n.a. (\geq 20)			Reduction in the most rostral C1 (rostrum) and the most occipital C5 (splenium) subregions of CC in AD patients compared with HC.	
	n 4 AD moderate	n.a. \pm n.a. ($<$ 20 - \geq 10)				
	n 6 AD severe	n.a. \pm n.a. ($<$ 10)				
	-22 HC	29.8 \pm 0.4 (n.a.)				
Teipel et al. (1998)	-20 AD:	12.2 \pm 10.2 (n.a.);	0.5 T magnet. A T1-weighted volumetric scan (slice thickness = 2 mm)	Hampel splitting	Absolute mean total callosal area was smaller in AD patients compared with HC.	
	n 7 AD mild	n.a. \pm n.a. (\geq 20)			Reduction of most rostral C1 and C2 (rostrum and anterior body) and of most caudal C5 (splenium) subregions of CC in AD patients compared with HC.	
	n 5 AD moderate	n.a. \pm n.a. ($<$ 20 - \geq 10)				
	n 8 AD severe	n.a. \pm n.a. ($<$ 10)				
	-21 HC	29.7 \pm 0.5 (n.a.)				
Teipel et al. (1999)	-12 AD:	12.5 \pm 10.0 (n.a.);	Two MRI sequences: -0.5 T magnet. A T1-weighted volumetric scan (slice thickness = 2.5 mm); -0.5 T magnet. A T1-weighted volumetric scan (slice thickness = 2 mm)	Hampel splitting	Absolute mean total callosal area was smaller in AD patients compared with HC.	
	n 3 AD mild	n.a. \pm n.a. ($>$ 20)			Reduction in most rostral C1 and C2 (rostrum and anterior body) and in most occipital C5 (splenium) subregions of CC in AD patients compared with HC.	
	n 5 AD moderate	n.a. \pm n.a. ($<$ 20 - \geq 10)				
	n 4 AD severe	n.a. \pm n.a. ($<$ 10)				
	-15 HC	29.7 \pm 0.5 (n.a.)				

Table 1, continued

Study (year)	Sample	MMSE mean \pm SD (range)	MRI acquisition	ROI method	Positive findings	Negative findings
Teipel et al. (2002)	-21 AD: n 9 AD mild n 10 AD moderate n 2 AD severe -10 HC	17.4 \pm 6.7 (1-28): n.a. \pm n.a. (≥ 20) n.a. \pm n.a. (≥ 10 - ≤ 20) n.a. \pm n.a. (< 10) 29.8 \pm 0.4 (29-30)	0.5 T magnet. A T1-weighted volumetric scan (slice thickness = 2 mm)	Hampel splitting	Cross-sectional study results: i) absolute mean total callosal area was smaller in AD patients compared with HC; ii) atrophy in rostrum and genu (C1) and isthmus and splenium (C5) of CC in AD patients compared with HC. Longitudinal study results: percentage rates of change in total CC and callosal subregion, rostrum and genu (C1) and isthmus and splenium (C5) of CC in AD patients compared with HC (analysis performed on a subgroup of AD matched with HC for observation time).	
Teipel et al. (2003)	-27 AD: n 9 AD mild n 9 AD moderate n 9 AD severe -28 HC	13.4 \pm 8.8 (0-27): n.a. \pm n.a. (≥ 20) n.a. \pm n.a. (< 20 - ≥ 10) n.a. \pm n.a. (< 10) 29.8 \pm 0.4 (29-30)	0.5 T magnet. A T1-weighted volumetric scan (slice thickness = 2 mm)	Hampel splitting	Total callosal size was smaller in AD patients compared with HC. Atrophy in rostrum and genu (C1) and isthmus and splenium (C5) of CC in AD patients compared with HC. Atrophy in splenium of CC was present even in mild AD patients compared with HC.	
Pantel et al. (1998)	-32 AD -17 VD -13 HC	163 \pm 6.4 (n.a.) n.r. 29.3 \pm 0.8 (n.a.)	1.5 T magnet. A T1-weighted volumetric scan (slice thickness = 1.2 \times 1.2 \times 1.5 mm)	Weis splitting Five mid-sagittal slices of CC were used.	Total size of CC and the most rostral part of CC (C1 = genu and rostrum; C2 = rostral body) were significantly smaller in AD patients compared with HC.	
Pantel et al. (1999)	-38 AD -20 HC	16.6 \pm 6.9 (n.a.) 29.2 \pm 0.6 (n.a.)	1.5 T magnet. A T1-weighted volumetric scan (slice thickness = 1.2 \times 1.2 \times 1.5 mm)	Weis splitting. Three mid-sagittal slices of CC were used.	Total size of CC and the five measured regional subsections of CC (rostrum and genu, anterior body, mid body, isthmus and splenium) were significantly smaller in AD patients compared with HC.	
Ortiz Alonso et al. (2000)	-23 AD -24 HC	16.9 \pm 2.4 (n.a.) 29.0 \pm 0.9 (n.a.)	1.5 T magnet. A T1-weighted volumetric scan (slice thickness = 1 mm)	Weis splitting	Reduction of CC2 (anterior body), CC3 (mid body) and CC4 (isthmus) in AD patients compared with HC.	
Hensel et al. (2002)	-23 AD -27 questionable dementia patients -33 HC	22.0 \pm 1.8 (n.a.) 26.0 \pm 1.8 (n.a.) 28.9 \pm 0.8 (n.a.)	1.5 T magnet. A T1-weighted volumetric scan (slice thickness = 0.9 \times 0.9 \times 1.5 mm)	Weis splitting	Reduction of total callosal size in AD patients compared with HC.	No CC segment was particularly atrophied in AD patients compared with HC. No statistically significant differences were found between patients with questionable dementia and any other group.

Table 1, continued

Study (year)	Sample	MMSE mean \pm SD (range)	MRI acquisition	ROI method	Positive findings	Negative findings
Hensel et al. (2004)	-12 AD: n 9 AD mild n 3 AD moderate -2 FTD -12 HC	23 \pm 2.1 (20-26); n.a. n.a. n.r. 28.5 \pm 1.3 (25-30)	Three MRI sequences and tomography: -1.5 T magnet. A T1-weighted volumetric scan (slice thickness = 0.9 \times 0.9 \times 1.5 mm) -1.5 T magnet. A T1-weighted volumetric scan (slice thickness = 0.9 \times 0.9 \times 1 mm) -3 T magnet. A T1-weighted volumetric scan (slice thickness = 1.5 mm)	Weis splitting	Total callosal area was reduced in AD patients compared with HC.	No specific subregion atrophy in CC in AD patients compared with HC.
Wiltshire et al. (2005)	-16 AD -24 PD -25 PDD -27 HC	21.0 \pm 8.2 (n.a.) n.r. n.r. 29.0 \pm 1.2 (n.a.)	Two MRI sequences: -1.5 T magnet. A T1-weighted volumetric scan (slice thickness = 5 mm) -1.5 T magnet. A T1-weighted volumetric scan (slice thickness = 5 mm)	Weis splitting	Total callosal area was reduced in AD patients compared with HC.	
Hensel et al. (2005)	-35 questionable dementia patients -39 HC	26.2 \pm 1.8 (n.a.) 28.9 \pm 1.1 (n.a.)	1.5 T magnet. A T1-weighted volumetric scan (slice thickness = 0.9 \times 0.9 \times 1.5 mm)	Weis splitting		No specific callosal subregion atrophy in questionable dementia patients compared with HC.
Thomann et al. (2006)	-10 AD -21 MCI "all subtypes" -21 HC	19.2 \pm 3.8 (n.a.) n.a. n.a.	1.5 T magnet. A T1-weighted volumetric scan (slice thickness = 0.98 \times 0.98 \times 1.8 mm)	Weis splitting	Total callosal area was reduced in AD and MCI patients compared with HC. Reduction in rostral subregions C1 (rostrum and genu), C2 (anterior body) and C3 (midbody) of CC in AD patients compared with HC. Reduction in rostral subregions C1 (rostrum and genu) and C2 (anterior body) of CC in MCI patients compared with HC.	
Wang PJ et al. (2006)	-22 AD -28 amnesic MCI -28 subjective cognitive complaints -50 HC	24.6 \pm 2.7 (n.a.) 27.3 \pm 2.2 (n.a.) 28.9 \pm 1.1 (n.a.) 29.1 \pm 1.2 (n.a.)	1.5 T magnet. A T1-weighted volumetric scan (slice thickness = 1.5 mm)	Weis splitting	Reduction in total callosal area in each group (AD, MCI and subjective cognitive complaints subjects) compared with HC. Reduction in posterior subregions C4 (isthmus) and C5 (splenium) in AD patients compared with HC. Reduction in posterior subregion C5 (splenium) in MCI and subjective cognitive complaints subjects compared with HC.	

Table 1, continued

Study (year)	Sample	MMSE mean \pm SD (range)	MRI acquisition	ROI method	Positive findings	Negative findings
Li et al. (2008)	-19 AD -20 HC	18.9 \pm 3.9 (n.a.) 29.5 \pm 0.9 (n.a.)	1.5 T magnet. A T1-weighted volumetric scan (slice thickness = 1.8 mm)	Weis splitting	Reduction in all five subregions of CC (rostrum and genu, anterior body, mid body, isthmus and splenium) in AD patients compared with HC.	
Thompson et al. (1998)	-10 AD -10 HC	19.7 \pm 5.7 (n.a.) 28.8 \pm 1.0 (n.a.)	1.5 T magnet. A T1-weighted volumetric scan (slice thickness = 1 mm)	Midsagittal slice of CC was split into 5 distinct sectors of equal percentage (20%) along a line joining the most anterior and posterior points of genu and splenium respectively [127,128].	Reduction in posterior "midbody" (corresponding mainly to the isthmus) of CC in AD patients compared with HC.	
Hanyu et al. (1999a)	-23 AD: n 6 AD n 13 AD n 4 AD -16 HC	n.a.: n.a. \pm n.a. (≥ 21) n.a. \pm n.a. (20-11) n.a. \pm n.a. (≤ 10) n.a. \pm n.a. (< 28)	1.5 T magnet. A T2-weighted image (section thickness 8 mm)	CC was split into four parts of equal size: anterior portion (rostrum and genu), middle portion (body) and posterior portion (isthmus and splenium) of CC.	Total callosal area was reduced in AD patients compared with HC. Atrophy of posterior subregions (isthmus and splenium) of CC in AD patients compared with HC.	
Yamauchi et al. (2000)	-16 AD -11 FTD -9 PSP -23 HC	19 \pm 5 (n.a.) n.r. n.r. 29 \pm 1 (n.a.)	1.5 T magnet. A T1-weighted volumetric scan (slice thickness = 3 mm)	CC was split into four parts of equal size: anterior (rostrum), middle-anterior, middle-posterior, and posterior (splenium).	Total callosal area was smaller in AD patients compared with HC. Reduction of the posterior quarter area (splenium) in AD patients compared with HC.	
Wang H. et al. (2006)	-13 amnesic MCI -13 HC	n.a. n.a.	1.5 T magnet. A T1-weighted volumetric scan (slice thickness = 1.5 mm)	Manual tracing of ROI of whole CC in midsagittal section.	No callosal atrophy in MCI patients compared with HC.	
Hallam et al. (2008)	-78 AD -28 MA -55 VD -20 HC	17.3 \pm 6.8 (n.a.) 25.9 \pm 1.7 (n.a.) n.r. 28.2 \pm 2.1 (n.a.)	0.5 T magnet. A T1-weighted volumetric scan (slice thickness = 5 mm)	The methodology derived 99 callosal widths based on an algorithm that divided each dorsal and ventral CC perimeter into 100 equidistant points and connected the corresponding numbered points between the dorsal and ventral surfaces of the CC. Subregions of CC were then identified by a factor analysis of these widths.	No CC regional differences between MA group and controls, but a trend for the region (W2-12 and W13-14) to be smaller in this patient group ($p = 0.05$). No significant CC regional differences between patient groups after correcting for multiple comparisons.	
Zarei et al., (2009)	-16 AD mild -13 VaD -22 HC	22.9 \pm 3.2 (n.a.) n.r. 28.7 \pm 1.4 (n.a.)	1.5 T magnet. A T1-weighted volumetric scan (slice thickness = 1 \times 1.5 \times 1 mm)	Probabilistic tractography to parcel the CC into 7 subregions according to its connectivity with major cerebral	No significant difference in total CC volume or in volume of CC subregions in AD	

Table 1, continued

Study (year)	Sample	MMSE mean \pm SD (range)	MRI acquisition	ROI method	Positive findings	Negative findings
Di Paola et al. (2010); Epub 2010a).	-30 AD: n 10 AD severe -20 AD mild -20 amnesic MCI -20 HC	n.a.: 10.7 \pm 3.7 (n.a.) 22.0 \pm 2.5 (n.a.) 27.1 \pm 2.5 (n.a.) 29.1 \pm 0.9 (n.a.)	3 T magnet. A T1-weighted volumetric scan (slice thickness = 1 \times 1 \times 1 mm)	cortex: prefrontal cortical region, M1, S1, premotor cortical region, posterior parietal cortical region, temporal, occipital cortical region. Mesh-based method: upper and lower callosal boundaries in midsagittal section of each brain were manually outlined. Then callosal upper and lower sections were redigitized to obtain 100 equidistant points. The spatial average from the 100 equidistant surface points representing the upper and lower boundaries was calculated resulting in a new midline segment, also consisting of 100 equidistant points. Finally, distances between 100 corresponding surface points between midline segment and upper and lower boundaries were quantified in mm.	Reduction in the splenium, anterior body and anterior third of CC in severe AD patients compared with HC.	patients compared with HC. No significant difference in CC in mild AD and amnesic MCI patients compared with HC.

Studies are grouped by the splitting method used.

AD = Alzheimer's disease.

CC = corpus callosum.

MA = mild ambiguous (patients with cognitive problems not severe enough for diagnosis of dementia [43]. They seem to be similar to MCI "all subtypes").

MCI = Mild Cognitive Impairment.

MID = multi-infarct dementia.

HC = healthy controls.

FTD = frontotemporal dementia.

PD = Parkinson's disease.

PDD = PD with dementia.

PSP = progressive supranuclear palsy.

Questionable dementia patients = are subjects typically suffering from mild forgetfulness. They are fully oriented and have no or slight impairment in social functions. They do not meet ICD-10 dementia criteria [45], and have a score of 0.5 in the Clinical Dementia Rating Scale (CDR) [58].

MMSE = Mini Mental Status Examination; mean (standard deviation).

VD = Vascular Dementia.

n.a. = data not available in the article.

n.r. = data available in the article for different pathology, therefore not reported.

Table 2
VBM studies of CC

Study (year)	Sample	MMSE mean \pm SD (range)	MRI acquisition	VBM method	Positive findings	Negative findings
Good et al. (2002)	-10 AD	21.2 \pm 5.0 (n.a.)	1.5 T magnet. A T1-weighted volumetric scan (slice thickness = 1.5 mm)	Optimized VBM using custom template, with SPM99	Presence of diffuse white matter atrophy within CC in AD patients compared with HC (however, the finding was not detailed to ascertain the location of peak foci of CC atrophy).	No difference in CC in MCI patients compared with HC.
	-10 SD	n.r.				
	-10 HC	29.8 \pm 0.4 (n.a.)				
Thomann et al. (2006)	-10 AD	19.2 \pm 3.8 (n.a.)	1.5 T magnet. A T1-weighted volumetric scan (slice thickness = 0.98 \times 0.98 \times 1.8 mm)	Standard VBM with SPM99	Reduction of CC volume in posterior part of C1 (genu) and anterior part of C2 (anterior body) in AD patients compared with HC.	No difference in CC in MCI patients compared with HC.
	-21 MCI "all subtypes"	n.a.				
	-21 HC	n.a.				
Chaim et al. (2007)	-14 AD:	20.7 \pm 3.1 (n.a.):	1.5 T magnet. A T1-weighted volumetric scan (slice thickness = 1.2 \times 1.2 \times 1.2 mm)	Optimized VBM using custom template, with SPM2. Analysis restricted to VOI of CC	Reduction of CC volume in rostral portion of left genu, in anterior and posterior portions of left and right CC body and in left splenium and isthmus in AD patients compared with HC.	No difference in CC in MCI patients compared with HC.
	n 11 AD	n.a. \pm n.a. (\leq 20)				
	n 3 AD	n.a. \pm n.a. (18-14)				
	-14 HC	29.1 \pm 0.5 (n.a.)				
Li et al. (2008)	-19 AD	18.9 \pm 3.9 (n.a.)	1.5 T magnet. A T1-weighted volumetric scan (slice thickness = 1.8 mm)	Optimized VBM using custom template, with SPM99	Reduction of CC volume in left isthmus and splenium in AD patients compared with HC.	No difference in CC in MCI patients compared with HC.
	-20 HC	29.5 \pm 0.9 (n.a.)				
Di Paola et al. (2010; 2010a)	-30 AD:	n.a.:	3 T magnet. A T1-weighted volumetric scan (slice thickness = 1 \times 1 \times 1 mm)	VBM with unified segmentation algorithm in SPM5. Analysis restricted to VOI of CC.	Reduction of CC density in genu, anterior body and splenium of CC was found in severe AD patients compared with HC.	No CC difference in mild AD patients compared with HC. No CC difference in amnesic MCI patients compared with HC.
	n 10 severe AD	10.7 \pm 3.7 (n.a.)				
	n 20 mild AD	22.0 \pm 2.5 (n.a.)				
	-20 amnesic MCI	27.1 \pm 2.5 (n.a.)				
	-20 HC	29.1 \pm 0.9				
Di Paola et al. (2010b)	-38 AD:	22.6 \pm 2.9 (n.a.)	3 T magnet. A T1-weighted volumetric scan (slice thickness = 1 \times 1 \times 1 mm)	VBM-DARTEL Analysis restricted to VOI of CC.	Reduction of CC density in genu and splenium of CC in mild AD patients compared with HC. Reduction of CC density in genu in amnesic MCI patients compared with HC.	No difference in CC in MCI patients compared with HC.
	-38 amnesic MCI	27.0 \pm 2.0 (n.a.)				
	-40 HC	29.2 \pm 1.2 (n.a.)				

The studies are presented in chronological order by publishing date.

AD = Alzheimer's disease.

CC = corpus callosum.

HC = healthy controls.

MCI = mild cognitive impairment.

MMSE = Mini Mental Status Examination; mean (standard deviation).

SD = semantic dementia.

VBM = Voxel-Based Morphometry.

VOI = volume of interest.

n.a. = data not available in the article.

n.r. = data available in the article for different pathology, therefore not reported.

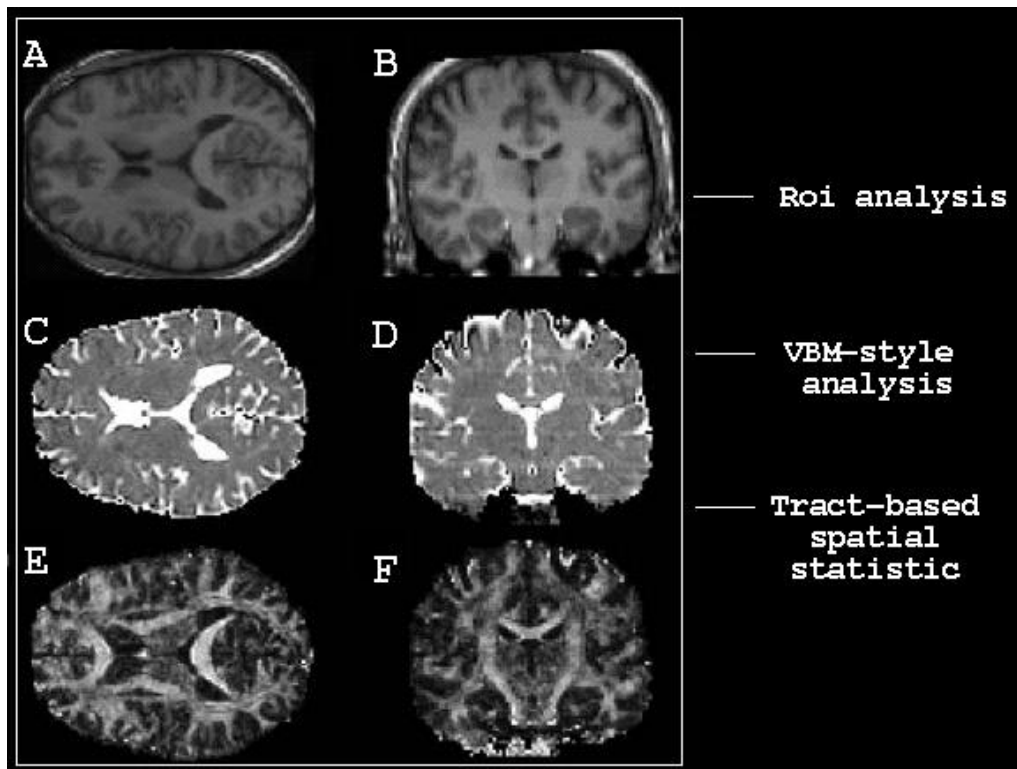


Fig. 4. Diffusion tensor-based images. A and B show axial and coronal T1-weighted anatomical images. C and D trace ADC maps (mean diffusivity) of the same slices shown in A and B. E and F are fractional anisotropy maps showing high contrast between gray and white matter. Once the mean diffusivity and fractional anisotropy maps are calculated, there are three approaches for post processing: manual ROI, VBM-style analysis [64] and tract-based spatial statistics (TBSS) [122].

down of tissue cytoarchitecture [68,69], sclerosis [70], or demyelinating processes [71–74]. Recently, Choi and colleagues [75] began investigating other measures of diffusion, such as radial diffusivity (DR) and axial diffusivity (DA), to determine whether differences in anisotropy are caused by diffusion perpendicular or parallel to the WM fibers, respectively. The assumption, arising out of experiments on animal models, is that significantly reduced DR in WM without differences in DA might represent specifically compromised integrity of myelin in the absence of axonal structural irregularities.

With respect to structural MRI (ROI and VBM), DWI and DTI techniques have the advantage of being very sensitive in detecting microstructural abnormalities not revealed by other volumetric measures [28,76]. In fact, structural MRI techniques, which reflect macrostructural changes, may not be sensitive to the degeneration of myelin and axons in the WM microstructure [28,46]. On the contrary, DWI and DTI parameters have been applied in CC studies and have demonstrated much greater sensitivity in revealing the WM degeneration in

AD than conventional MRI imaging techniques [68,71,77].

DWI studies on AD “all stages” patients [30,33] report no significant group differences in measurements of the anisotropy index (AI) – calculated by dividing the ADC perpendicular to the prominent callosal fiber direction by the ADC parallel to the predominant fiber direction of the CC – within the genu and splenium of the CC. On the other hand, Hanyu et al. [28,29] using the same type of AI (that the authors called ADC ratio) found a decrease in the anterior (rostrum and genu) and posterior (isthmus and splenium) CC of AD “all stages” patients. Also, Wang and collaborators and Ray and colleagues [46,78] found a higher ADC in the CC of patients with amnesic MCI than in HC.

DTI studies on AD “all stages” patients [32,35,36,39,41,79,80] basically found changes in the anterior (genu) and posterior (splenium) subregions of the CC in AD patients compared with HC. More specifically, Rose et al. [32] found a value reduction in the splenium of AD patients but not in HC. They used lattice index (LI) as a measure of anisotropy. LI is an intervoxel

measurement of diffusion anisotropy that exploits information about the orientation coherence of the eigenvectors of diffusion tensor in adjacent voxels, to improve the estimate of diffusion anisotropy within a reference voxel. It is especially immune to background noise in the DW images and provides a quantitative, robust measurement of diffusion anisotropy [81].

The other studies that measured MD and/or FA can be separated into those which found mainly an increase of MD and/or a decrease of FA in the posterior subregion (splenium) of the CC in AD [35,36,41,79,80] and those which reported an increase in MD or a decrease in FA in the anterior subregions (genu and anterior body) of CC in AD compared with HC [35,39]. It is very difficult to summarize the general picture of these results because other studies on AD “all stages” [23,37,40,75] reported no significant differences in MD or FA in the anterior and posterior CC when the patient group was compared with HC. Stahl and coworkers [40] also measured ADC and relative anisotropy and found no differences between AD patients and HC. Furthermore, the findings of studies on more homogeneous patients, such as those with mild AD, are discrepant. For example, Xie et al. [82] found a decrease of FA in the genu and left anterior body of the CC, whereas Ulkmar et al. [83] found a decrease of FA in the genu and splenium of the CC; other studies [84–87] found no differences in the CC in patients with mild AD.

At present, the DTI study results on MCI patients can be divided into two groups: 1) DTI studies on both amnesic and MCI “all subtypes” [23,40,41,84,85,88] that found no differences in MD and/or in FA in the CC compared with HC; and 2) the most recent studies [83,86,89–91], which reported differences. One study on MCI “all subtypes” [89] found a significant change in MD and FA in the genu and the splenium of the CC in patients compared with HC. Moreover, studies on amnesic MCI [83,86,90] mainly found a decreased FA and/or increased MD value in the splenium of the CC. Wang and colleagues [91] also reported a decreased FA value in the genu and the splenium and increased ADC in the genu of the CC (see Table 3 for technical details of the study). In our study [21], we found reduced FA in the genu and anterior body of the CC, increased DA in the body and in the posterior subregions of the CC, and increased DR in the entire CC in patients with mild AD compared with HC. We found no significant differences in the CC in patients with amnesic MCI compared with HC.

DISCUSSION

The purpose of this review was to summarize CC changes in patients with AD and MCI with regard to different illness stages and the measurements used to calculate the modifications. Regardless of the technique used (i.e., ROI, VBM, DWI, or DTI), the main result in AD patients across all studies when severity of illness was not taken into consideration (AD “all stages”) was primarily a change in the anterior (genu and anterior body) and posterior (isthmus and splenium) regions of the CC (see Table 4). This finding is less consistent when patients are separated into more homogeneous groups (e.g., mild AD and amnesic MCI). Indeed, some studies reported changes in the anterior subregion (e.g. [20,21,46,82]), some in the posterior subregion [20,21,83,91], and some found no callosal changes [40,85,92]. This inconsistency in results may be the consequence of reduced sample size of studies considering discrete diagnostic categories of different clinical stages. But, whatever the reason, little is known about how early callosal atrophy occurs in AD and whether this change is already detectable in patients at higher risk of developing the disease, such as those with amnesic MCI [51] (see Table 4).

Region-specific callosal reduction

In summary, callosal atrophy in AD “all stages” affects the posterior and anterior subregions and spares the body of the CC. Therefore, the CC atrophy found in AD “all stages” groups corresponds with previously reported cortical areas considered to be involved in AD pathology [93]. The posterior subregion (splenium and isthmus) subserves two-thirds of the higher-order processing areas of the lateral temporal and parietal lobe, which, together with the mesial temporal structures [94], are primarily involved in cortical AD degeneration [93,95,96]. This could interfere with functioning of the posterior cortical memory networks, which subserve episodic memory operations and are impaired early in AD patients [97]. On the other hand, the anterior portion (genu and anterior body) is responsible for the inter-hemispheric connection between the prefrontal association cortices [87,98,99], that is, the regions involved in the later stages of AD pathology evolution [93,95,96] and implicated in monitoring information in working memory and in the active retrieval of information from posterior cortical association areas [100–102]. Thus, the volume reduction in these

Table 3
DWI and DTI studies of CC

Study (year)	Sample	MIMSE mean \pm SD (range)	MRI acquisition	Method	Positive findings	Negative findings
<i>DWI studies</i>						
Sandson et al. (1999)	-10 AD -11 HC	n.a. n.a.	1.5 T magnet; three-direction diffusion-weighted sequences obtained with EPI technique; slice thickness 7 mm, no interslice gap	ROIs were manually drawn on T2-weighted images, using characteristic landmarks and standard atlases and were transferred onto the corresponding ADC maps. ROIs were placed in the genu and splenium. ROIs were of varying sizes (10–15 pixels).	Although AI was higher in anterior in splenium of CC in AD group compared with HC, this finding was not significant.	No difference was found in AI in genu of CC in AD patients compared with HC.
Hanyu et al. (1999a)	-23 AD: n 6 AD n 13 AD n 4 AD -16 HC	n.a.: n.a. \pm n.a. (≥ 21) n.a. \pm n.a. (20–11) n.a. \pm n.a. (≤ 10) n.a. \pm n.a. (≤ 28)	1.5 T magnet; two-direction diffusion-weighted sequences obtained with EPI technique; slice thickness 8 mm with interslice gap	ROIs were manually drawn on T2-weighted reversed images; ROIs were placed in the genu and splenium. ROIs were of varying sizes (10–15 pixels). ROIs were placed in the anterior portion (rostrum and genu), in middle portion (body) and in posterior portion (isthmus and splenium) of CC. Circular ROIs were of varying sizes (4–6 mm in diameter).	ADC was higher in anterior (rostrum and genu) and posterior (isthmus and splenium) subregions of CC in AD patients compared with HC.	
Hanyu et al. (1999b)	-10 AD 14 VDBT -20 HC	13.4 \pm 4.3 (n.a.) n.r. 29.3 \pm 0.9 (n.a.)	1.5 T magnet; two-direction diffusion-weighted sequences obtained with EPI technique; slice thickness 8 mm with interslice gap	ROIs were manually drawn on T2-weighted images; ROIs were placed in genu and splenium of CC. Circular ROIs were of varying sizes (4–6 mm in diameter).	ADC in genu and splenium of CC were significantly higher in AD patients compared with HC.	
Bozzao et al. (2001)	-18 probable AD -16 Po/Pr AD -15 HC	17.1 \pm 3.1 (n.a.) 27.2 \pm 2.2 (n.a.) 29.4 \pm 1.2 (n.a.)	1.5 T magnet; three-direction diffusion-weighted sequences obtained with EPI technique; slice thickness 6 mm with interslice gap	ROIs were drawn manually on ADC maps; they were placed in genu and splenium of CC and were of fixed size (50 pixels).	Measurements of AI within genu and splenium of CC did not disclose any significant group difference.	
Wang H et al. (2006)	-13 amnesic MCI -13 HC	n.a. n.a.	1.5 T magnet; three-direction diffusion-weighted sequences obtained with EPI technique; slice thickness 6 mm with interslice gap	ROIs were defined manually on T1-weighted images. Then T1-weighted images were coregistered to the DWI images. The transformation matrices obtained were used to map each ROI onto ADC maps; ROIs included the whole CC in midsagittal section.	ADC was increased in CC in MCI patients compared with HC.	
Ray et al. (2006)	-13 amnesic MCI -13 HC	26.8 \pm 2.6 (n.a.) 28.6 \pm 0.8 (n.a.)	1.5 T magnet; three-direction diffusion-weighted sequences obtained with EPI technique; slice thickness 6 mm with interslice gap	ROIs were defined manually on the T1-weighted image. Then T1-weighted images first coregistered to the ADC maps; so the ROIs were mapped onto the ADC maps; ROIs included the whole CC in midsagittal section.	ADC was higher in the CC in MCI patients compared with HC.	

Table 3, continued

Study (year)	Sample	MMSE mean \pm SD (range)	MRI acquisition	Method	Positive findings	Negative findings
<i>DTI studies</i>						
Rose et al. (2000)	-11 AD -9 HC	n.a. \pm n.a. (6-21) n.a. \pm n.a. (> 28)	1.5 T magnet; six-direction diffusion-weighted sequences obtained with EPI technique; slice thickness 5 mm with interslice gap	The lattice index (LI) was used as a quantitative measure of anisotropy in DTI; ROI was manually traced in splenium of CC using color coding map to identify the region. Size of ROI n.a.	LI of splenium of CC was less in AD patients than in HC. Also, in a subgroup of AD patients with mild to moderate probable AD (MMSE 17-21), LI of splenium was less than in HC.	
Bozzali et al. (2002)	-16 AD -10 HC	n.a. \pm n.a. (9.3-25.4) median 19.4 n.a. \pm n.a. (26.8-30.7) median 28.6	1.5 T magnet; eight-direction diffusion-weighted sequences obtained with EPI technique; slice thickness 5 mm with interslice gap	ROIs were sampled manually on three consecutive slices in genu and splenium of CC. Rectangular ROI of variable size (range = 11.4-46.7 mm ²) (the exact ROI size used for CC is n.a.).	MD was higher and FA lower in CC of AD patients compared with HC.	
Takahashi et al. (2002)	-10 AD -10 HC	19.0 \pm 3.2 (n.a.) n.a.	3 T magnet; six-direction diffusion-weighted sequences obtained with EPI technique; slice thickness 6 mm with interslice gap	ROIs were defined manually on anatomical T2-weighted image. ROIs were placed in posterior portion (splenium) of CC in AD patients compared with HC.	Reduction in FA values in posterior portion (splenium) of CC in AD patients compared with HC.	
Head et al. (2004)	-25 AD -25 non demented older adults -25 younger HC	22.9 \pm 4.7 (15-30) 28.9 \pm 1.2 (26-30) n.a.	1.5 T magnet; four+three-direction diffusion-weighted sequences obtained with EPI technique; slice thickness 4 mm, no interslice gap	ROIs were manually outlined on the anisotropy image of each subject. ROIs of anterior (genu and rostrum) and posterior CC (splenium) consisted of 21 slices of CC.	Decreased FA in anterior and posterior CC in AD patients compared with younger adults (aging effect). Increased MD in callosal regions (anterior and posterior) in AD patients and non demented older adults compared with younger adults.	No significant difference in MD and FA in anterior and posterior CC in AD patients compared with non demented older adults.
Fellgiebel et al. (2004)	-19 AD -14 amnesic MCI -10 HC	18.3 \pm 4.8 (n.a.) 24.6 \pm 2.7 (n.a.) 24.6 \pm 1.3 (n.a.)	1.5 T magnet; six-direction diffusion-weighted sequences obtained with EPI technique; slice thickness 5 mm, no interslice gap	ROIs were defined manually on the anatomical T2-weighted image (b = 0 s/mm ²) and then transferred to FA and MD index maps. ROIs were of varying sizes (15-25 pixels) in genu and splenium of CC.	No difference in FA or MD were found in CC of AD and MCI patients compared with HC. No differences were found between MCI and AD patients regarding MD and FA values when the two groups were compared.	

Table 3, continued

Study (year)	Sample	MMSE mean \pm SD (range)	MRI acquisition	Method	Positive findings	Negative findings
Sugihara et al. (2004)	-20 probable AD	n.a.	1.5 T magnet; six-direction diffusion-weighted sequences obtained with EPI technique; slice thickness 5 mm with interslice gap.	ROIs in genu and splenium of CC were placed in T2-weighted image. Fixed-sized ROIs (6 pixels).	No differences in FA were found in CC in AD patients compared with HC.	
	-20 VD	n.a.				
	-10 HC	n.a.				
Choi et al. (2005)	-10 AD	25.2 \pm 2.5 (19-27)	1.5 T magnet; six-direction diffusion-weighted sequences obtained with EPI technique; slice thickness n.a.	ROIs were defined manually on anatomical T2-weighted image ($b = 0$) of DTI data so that coregistration between different image acquisition methods was no longer necessary. Small-sized (area = 11.4 mm ²) circular ROIs were placed in genu and splenium of CC.	No differences in FA, MD, DR and DA within genu and splenium of CC in AD patients compared with HC.	
	-10 HC	29.5 \pm 1.1 (27-30)				
Duan et al. (2006)	-16 AD	13 \pm n.a. (8-22)	1.5 T magnet; twenty-five-direction diffusion-weighted sequences obtained with EPI technique; slice thickness 5 mm, no interslice gap	Circular ROIs (of 20-40 mm ²) were placed in genu and splenium of CC. The genu and splenium of CC were sampled at the slices of the optic chiasm and anterior part of the inferior colliculus, respectively.	Decreased FA and increased MD were found in splenium of CC in AD patients compared with HC.	
	-12 HC	28 \pm n.a. (27-30)				
Medina et al. (2006)	-14 AD	24.5 \pm 1.9 (n.a.)	1.5 T magnet; six-direction diffusion-weighted sequences obtained with EPI technique; slice thickness 6 mm, no interslice gap	Voxel-based analysis: the T2 images were spatially normalized to a standard T2 template in SPM99. Parameters from this transformation were then applied to the DT images and statistical maps were created for DW and FA values. To limit the analysis to DW and FA values in white matter, an individual subject mask volumes were created, which were used to exclude voxels of no interest. The individual white matter masks were then applied to individual subject DW and FA maps. Group differences in voxel level DTI values were assessed using these individual, masked DW and FA maps.	No differences were found in FA or in MD in CC in AD and MCI patients compared with HC.	
	-16 amnesic MCI	26.9 \pm 2.1 (n.a.)				
	-21 HC	29.3 \pm 0.7 (n.a.)				
Naggara et al. (2006)	-12 AD	27 \pm 2.7 (20-30)	1.5 T magnet; twenty-five-direction diffusion-weighted sequences obtained with EPI technique; slice thickness 5 mm, no interslice gap	ROIs were defined manually on the anatomical T2-weighted image ($b = 0$) and then transferred onto MD and FA maps. Circular ROIs of variable sizes (mean: 40 mm ²) were placed in genu and splenium of CC.	Decreased FA and increased MD were found in splenium of CC in AD patients compared with HC.	
	-12 HC	29.8 \pm 0.4 (20; 30)				

Table 3, continued

Study (year)	Sample	MMSE mean \pm SD (range)	MRI acquisition	Method	Positive findings	Negative findings
Xie et al. (2006)	- 13 AD - 16 HC	21.1 \pm n.a. (19-24) n.a. \pm n.a. (> 27)	1.5 T magnet; thirteen-direction diffusion-weighted sequences obtained with EPI technique; slice thickness 4 mm, no interslice gap	Voxel-based analysis: the b0 images of all control subjects and patients were normalized to the standard EPI template of SPM2. Then the FA maps were normalized by applying the normalization parameters determined from the normalization of the b0 images. Because misregistration of FA maps can lead to falsepositive results, a mask was used to exclude those clusters of no interest (FA no more than 0.3).	Decreased FA in genu and left anterior body of CC was found in AD patients compared with HC.	
Rose et al. (2006)	- 17 amnesic MCI - 17 HC	26.1 \pm 2.2 (n.a.) 28.2 \pm 1.2 (n.a.)	1.5 T magnet; optimized diffusion tensor sequence; slice thickness 2.5 mm with interslice gap	Voxel-based analysis: the b0 images were normalized to the Montreal Neurological Institute template known as the ICBM152 to enable voxel-by-voxel statistical analysis of diffusivity indices between groups. Then the FA and MD maps were normalized by applying the normalization parameters determined from the normalization of the b0 images. A value of t4.095 was considered to be significant ($p = 0.001$). Voxels from the FA and MD maps with t4.096 were automatically extracted and classified as a ROI when > 20 voxels were contiguous.		No differences in FA and/or MD in CC were found in MCI patients compared with HC.
Stahl et al. (2007)	- 15 AD - 15 amnesic MCI - 19 HC	n.a. \pm n.a. (15-29) median 25 n.a. \pm n.a. (23-29) median 27 n.a. \pm n.a. (27-30) median 30	1.5 T magnet; six-direction diffusion-weighted sequences obtained with EPI technique; use of an 8-channel phased-array head coil and parallel imaging; slice thickness n.a.	ROIs were defined manually on the anatomical T2-weighted image ($b = 0 \text{ s/mm}^2$) and then transferred to the ADC, FA and RA maps. ROI placement approach (12-30 pixel size depending on the anatomical region) for genu and splenium of CC.	ADC increased and FA and RA decreased in splenium of CC in patients with AD compared with MCI patients.	No difference in ADC, FA and/or in RA in genu and splenium of CC in AD and MCI compared with HC.
Teipel et al. (2007)	- 15 AD - 14 HC	20.3 \pm 4.6 (17-28) 28.8 \pm 1.0 (27-30)	1.5 T magnet; six-direction diffusion-weighted sequences obtained with EPI technique; use of an 8-channel phased-array head coil and parallel imaging; slice thickness 3.6 mm, no interslice gap	Voxel-based analysis: normalization of FA maps to an anatomical template, resulting in FA maps projected into a standard space (i.e. a whole-brain voxel-based anatomic template) was used.	Decreased FA in anterior (genu) CC in AD patients compared with HC.	

Table 3, continued

Study (year)	Sample	MMSE mean \pm SD (range)	MRI acquisition	Method	Positive findings	Negative findings
Zhang et al. (2007)	- 17 AD - 17 MCI "all subtypes" - 18 HC	22.1 \pm 4.0 (n.a.) 27.9 \pm 2.0 (n.a.) 29.5 \pm 0.8 (n.a.)	1.5 T magnet; six-direction diffusion-weighted sequences obtained with EPI technique; slice thickness 5 mm, no interslice gap.	ROIs in the genu and splenium of CC; color maps to aid ROI placements; fixed-sized ROIs (from $4 \times 4 \text{ mm}^2$ to $6 \times 9 \text{ mm}^2$).	Decreased FA in splenium of CC in AD patients compared with HC. Decreased FA in splenium of CC in AD patients compared with MCI.	No difference in FA in genu and splenium in MCI patients compared with HC. No difference in MD in CC in AD and MCI patients compared with HC and compared with one other.
Damoiseaux et al. (2008)	- 16 AD - 8 amnesic MCI - 8 HC young - 22 HC old	22.9 \pm 3.2 (n.a.) 25.9 \pm 2.6 (n.a.) 29.5 \pm 0.5 (n.a.) 28.7 \pm 1.4 (n.a.)	1.5 T magnet; sixty diffusion directions and 10 images with no diffusion weighting sequences obtained with EPI technique. slice thickness 2 mm, no interslice gap	Analysis of FA data was carried out using TBSS on the whole WM.		No difference in FA in CC in either AD or MCI patients compared with HC.
Shim et al. (2008)	- 40 multi-domain amnesic MCI: n 21 nvMCI n 19 vMCI - 17 HC	n.a.: 24.5* \pm 2.5 (n.a.) 25.3* \pm 3.0 (n.a.) 28.7* \pm 1.1 (n.a.)	1.5 T magnet; twenty five-direction diffusion-weighted sequences obtained with EPI technique; slice thickness 5 mm, no interslice gap	Manual tracing of ROI; all ROIs were placed on each MR image using a standardized placement procedure with atlas-based rules for morphological landmarks. They were placed on the <i>b0</i> images and then superimposed over the identical slices on the FA and MD maps; sized ROI for CC: 25 mm^3 for genu and splenium.	Decreased FA and increased MD values in genu and splenium of CC in both types of MCI patients compared with HC.	
Ukmar et al. (2008)	- 14 mild AD - 15 amnesic MCI - 18 HC	23.4 \pm 2.8 (n.a.) 28.9 \pm 0.8 (n.a.) 29.9 \pm 0.2 (n.a.)	1.5-T magnet; thirty-two directions diffusion-weighted sequences obtained with EPI technique; slice thickness 2 mm with interslice gap	Manual placement of 0.8-cm^2 of ROI's allowed measuring fractional anisotropy in the white matter of genu and splenium of CC.	Decreased FA in genu and splenium of CC in AD patients compared with HC. Decreased FA in splenium of CC in MCI patients compared with HC.	
Cho et al. (2008)	- 11 amnesic MCI - 11 HC	24.9* \pm 2.4 (n.a.) 28.7* \pm 0.8 (n.a.)	1.5-T magnet; twenty five directions diffusion-weighted sequences obtained with EPI technique; slice thickness 4 mm, no interslice gap	A standardized placement procedure was used to place spherical ROI's using atlas-based rules with morphological landmarks by taken from Mori et al. [124] for each MRI. The voxel size of the ROI was determined as $7 \mu\text{L}$ voxel for the body of the CC; it was $25 \mu\text{L}$ voxel for genu and splenium of the CC.	Decreased FA in splenium of CC in MCI patients compared with HC. Increased MD in splenium of CC in MCI patients compared with HC.	
Parente et al. (2008)	- 15 possible AD - 20 probable AD - 25 amnesic MCI - 16 HC	24.5 \pm 0.5 (n.a.) 18.3 \pm 5.1 (n.a.) 28.0 \pm 1.1 (n.a.) 29.4 \pm \pm 0.9 (n.a.)	1.5-T magnet; six orthogonal directions diffusion-weighted sequences obtained with EPI technique; slice thickness 5 mm with interslice gap	Manual placement of 5 pixel circular ROI in splenium of CC.	Decreased FA in splenium of CC in MCI and probable AD patients compared with HC.	No difference in FA in possible AD patients compared with HC.

Table 3, continued

Study (year)	Sample	MMSE mean \pm SD (range)	MRI acquisition	Method	Positive findings	Negative findings
Zarei et al. (2009)	-16 mild AD -13 VaD -22 HC	22.9 \pm 3.2 (n.a.) n.r. 28.7 \pm 1.4 (n.a.)	1.5-T magnetic resonance imaging sixty diffusion directions diffusion-weighted sequences obtained with EPI technique; slice thickness 2 mm, no interslice gap	Analysis of FA data was carried out using TBSS. CC was divided into 7 subregions: prefrontal cortical (PFC), premotor cortical, M1, S1, posterior parietal cortical, temporal cortical, and occipital cortical.		no difference in FA between AD patients and HC.
Wang L. et al. (2009)	-10 amnesic MCI -10 HC	26.4 \pm 2.2 (n.a.) 29.7 \pm 0.5 (n.a.)	3 T magnetic resonance imaging; sixteen directions diffusion-weighted sequences obtained with EPI technique; slice thickness 2 mm; no interslice gap	Analysis of FA and ADC maps was carried out using FSL. ROIs were sampled manually on five consecutive slices in genu and splenium of CC.	Decreased FA in genu and splenium of CC in amnesic MCI patients. Increased ADC in genu of CC in amnesic MCI patients.	
Di Paola et al., (2010b)	-38 AD: -38 amnesic MCI -40 HC	22.6 \pm 2.9 (n.a.) 27.0 \pm 2.0 (n.a.) 29.2 \pm 1.2 (n.a.)	3 T magnetic resonance imaging; thirty diffusion directions diffusion-weighted sequences obtained with EPI technique. slice thickness 1.8 mm, no interslice gap.	Analysis of FA, DR and DA data was carried out using TBSS on the whole CC.	Decreased FA in genu and anterior body of CC; increased DA in body and posterior subregion of CC; and increased DR in the entire CC in mild AD subjects compared with HC.	No difference in FA, DR or DA between amnesic MCI patients and HC.

The studies are presented in chronological order by publishing date.

AD = Alzheimer's disease.

ADC = apparent diffusion coefficient (i.e. magnitude of water diffusion).

AI = anisotropy index.

CC = corpus callosum.

DA = axial diffusivity.

DR = radial diffusivity.

EPI = echo planar imaging sequence.

FA = fractional anisotropy.

HC = healthy controls.

LI = lattice index.

MCI = mild cognitive impairment.

MCI "all subtypes" = amnesic MCI and multiple-domain (both amnesic and/or non amnesic MCI).

MD = mean diffusivity.

MMSE = Mini Mental Status Examination; mean (standard deviation).

nvMCI = non-vascular mild cognitive impairment.

Po/Pr = Possible/Probable.

RA = relative anisotropy.

ROI = region of interest.

TBSS = tract-based spatial statistics.

VDBT = vascular dementia of the Binswanger type.

vMCI = vascular mild cognitive impairment.

n.a. = data not available in the article.

n.r. = data available in the article for different pathology, therefore not reported.

* = Korean Mini Mental State Examination [126].

Table 4

Summary of ROI, VBM, DWI, and DTI studies of patients with Alzheimer's disease and mild cognitive impairment since 1997 showing corpus callosum changes

Patients	Techniques	Studies	Total CC Area	Anterior CC	Body			Posterior CC	
					A	M	P		
AD "all stages"	ROI	Lyoo et al., (1997)		+	+	+	+	+	
		Hampel et al., (1998)	+	+				+	
		Teipel et al., (1998)	+	+	+			+	
		Thompson et al., (1998)						+	
		Pantel et al., (1998)	+	+	+				
		Hanyu et al., (1999b)	+					+	
		Teipel et al., (1999)	+	+	+			+	
		Pantel et al., (1999)	+	+	+	+		+	
		Yamauchi et al., (2000)	+					+	
		Black et al., (2000)	+	+	+		+	+	
		Teipel et al., (2002)	+	+				+	
		Teipel et al., (2003)	+	+				+	
		Hensel et al., (2004)							
		Thomann et al., (2006)	+	+	+	+			
		Tomaiuolo et al., (2007)	+	+	+	+		+	
	Li et al., (2008)		+	+	+		+		
	Hallem et al., (2008)	+	+				+		
	VBM	Good et al., (2002)	+						
		Thomann et al., (2006)			+				
		Chaim et al., (2007)			+	+	+	+	
		Li et al., (2008)						+	
		DWI	Sandson et al., (1999)						
			Hanyu et al., (1999a)			+			+
	Hanyu et al., (1999b)				+			+	
	DTI	Bozzao et al., (2001)							
		Rose et al., (2000)						+	
		Bozzali et al., (2002)			+			+	
		Takahashi et al., (2002)						+	
		Head et al., (2004)							
		Fellgiebel et al., (2004)							
		Sugihara et al., (2004)							
		Duan et al., (2006)						+	
		Stahl et al., (2007)							
Teipel et al., (2007)				+					
Zhang et al., (2007)							+		
Severe AD		ROI	Di Paola et al., (2010a)		+	+		+	
	VBM	Di Paola et al., (2010a)		+	+		+		
	DTI	Parente et al., (2008)					+		
Moderate AD	ROI	Ortiz Alonso (2000)			+	+	+		
Mild AD	ROI	Lyoo et al., (1997)					+	+	
		Hensel et al., (2002)	+				+	+	
		Teipel et al., (2003)						+	
		Hensel et al., (2005)							
		Wang PJ et al., (2006)	+					+	
		Zarei et al., (2009)							
		Di Paola et al., (2010a)							
		Di Paola et al., (2010a)							
		Di Paola et al., (2010b)			+			+	
		Bozzao et al., (2001)							
	VBM	DWI	Choi et al., (2005)						
		DTI	Medina et al., (2006)						
		Naggara et al., (2006)						+	
		Xie et al., (2006)			+	+			
		Damoiseaux et al., (2008)							
		Ulkmar et al., (2008)						+	
		Parente et al., (2008)							
		Zarei et al., (2009)							

Table 4, continued

Patients	Techniques	Studies	Total CC Area	Anterior CC	Body			Posterior CC
					A	M	P	
MCI "all subtypes"	ROI	Di Paola et al., (2010b)	+	+				+
		Thomann et al., (2006)	+	+	+			
		Hallem et al., (2008)						
	VBM	Thomann et al., (2006)						
Amnesic MCI	DTI	Zhang et al., (2007)						
		Shim et al., (2008)		+				+
	ROI	Wang H et al., (2006)	+					+
		Wang PJ et al., (2006)						
	VBM	Di Paola et al., (2010a)						
		Di Paola et al., (2010b)			+			
	DWI	Wang PJ et al., (2006)	+					
		Ray et al., (2006)	+					
	DTI	Fellgiebel et al., (2004)						
		Medina et al., (2006)						
		Rose et al., (2006)						
		Stahl et al., (2007)						
		Damoiseaux et al., (2008)						
Ulkmar et al., (2008)								+
Cho et al., (2008)								+
Parente et al., (2008)							+	
Wang L et al., (2009)				+			+	
Di Paola et al., (2010b)							+	

AD = Alzheimer's disease.

CC = corpus callosum.

MA = mild ambiguous (similar to MCI).

MCI = mild cognitive impairment.

Anterior CC = rostrum and genu.

Body (A = anterior; M = mid; P = posterior body).

Posterior CC = isthmus and splenium.

brain regions could account for general deficits in executive functions and attention in AD.

Finally, the body of the CC is most involved in motor and somato-sensory functions, which are usually spared in AD patients.

Possible underlying mechanisms

The basic assumption is that callosal atrophy in AD is the anatomical correlate of Wallerian degeneration of commissural nerve fibers. Therefore, it might show the same pattern of neocortical neurodegeneration. Based on the Wallerian degeneration hypothesis and on the AD neuronal degeneration pattern [103,104], the posterior CC subregions should be involved in the earlier stages of the disease and the anterior CC subregions only in the later stages. Nevertheless, several studies [20, 21,82,89] found that a reduction in the genu of the CC was already present in the early and preclinical stages of AD.

It has been recently suggested that myelin breakdown is an important component of the illness process

in AD [72,105,106]. According to this hypothesis, late-myelinating fibers should be more susceptible to myelin breakdown. The susceptibility of this subset of axons to myelin breakdown [107–110] may constitute an alternative mechanism through which the progression of cortical AD pathology occurs in the direction opposite to myelination [93], that is, the fibers that myelinate first in development are the last to be affected by AD and those that myelinate much later in normal development are the first to be affected by the AD degenerative process [72,106].

The CC contains late-myelinating fibers in the genu [98,99] and early-myelinating fibers in the splenium. Thus, it seems plausible to affirm that both Wallerian degeneration and myelin breakdown mechanisms are responsible for the region-specific illness effects. In this view, Wallerian degeneration affects the posterior CC subregion that receives axons directly from those brain areas (temporo-parietal lobe regions) that are primarily affected by AD pathology. Differently, the myelin breakdown process might affect the later-

myelinating CC subregion, causing changes in the genu of the CC already in the early stage of the disease.

We tested the hypothesis that both Wallerian degeneration and myelin breakdown might be responsible for the region-specific callosal change detected in the mild AD patients in our a VBM and DTI study [21]. We followed the assumption, arising out of experiments on animal models, that a reduction in DR might signify a loss of myelin integrity and that a reduction of DA might implicate axonal damage expected with Wallerian degeneration [71,73,74]. Our results [21] suggest that both these mechanisms affecting the callosal WM are present. Indeed, we found atrophy in posterior and anterior subregions of the CC already in the early stage of AD (mild AD) and in amnesic MCI (see VBM data). However, the atrophy seemed to be due to different factors (see DTI data). In the anterior CC, we found loss of the preference of water diffusion in fiber direction (decreased FA) and major diffusion in the direction perpendicular to the CC fibers (increased DR). A change in DR not mirrored by a similar change in DA (such as that observed in the anterior portion of the CC) would most probably be caused by specific damage to the myelin sheaths that restrict DR. Thus, these changes suggest a loss of myelin integrity, possibly due to a myelin breakdown mechanism. In the posterior CC subregion, we found an increase in water diffusion in the direction of the fibers (increased DA, no difference in FA). These changes suggest widespread tissue damage leading to a generalized increase in extracellular space due, for example, to the axonal atrophy expected with Wallerian degeneration.

Discrepancies with previous findings

The controversial results concerning regional atrophy of the CC are most likely due to the methods adopted across studies, such as the different criteria used to select patients, the different stages of illness considered, and the different number of participants. Regarding the criteria used to select patients, here we report only a few examples. Thomann and collaborators [10] defined MCI patients according to the Aging-associated Cognitive Decline (AACD) criteria [111], which have been demonstrated to capture a larger group of patients than the MCI criteria. They also included people with cognitive impairment of a non-amnesic nature [112] and assigned the diagnosis of MCI with higher probability [113]. Therefore, this MCI group [10] was clearly more heterogeneous than groups in other studies. Yamauchi et al. [14] studied AD with early onset, which

is considered a peculiar type of AD. In fact, it has been shown that AD patients with early onset have a typical and different topographical pattern of brain atrophy than patients with late onset AD, with possible consequences on CC subregion changes during the course of AD [114,115].

Furthermore, the different degree of AD severity in some previous samples may also have been responsible for discrepant results. Many studies included AD patients with different degrees of pathology, for example, from mild to severe [7,14,15] or from mild to moderate [8,10,42] (see Tables 1, 2, 3). Thus, results may have been biased by the presence of subjects at different illness stages.

We have to consider that the vast majority of studies are cross-sectional, comparing AD patients and controls. Thus, anatomical changes described in AD patients could have existed prior to the onset of the illness and considered as a risk factor in AD. To solve this issue, in the near future follow-up investigations are strongly required in order to clarify how CC changes longitudinally in preclinical and clinical AD.

Limitations of the techniques

In early studies, the CC was manually traced (ROI studies) and segmented according to common parcellation schemes, that is, according to Witelson [44], or Hampel [18] (see Table 1 and Fig. 2). These callosal segmentation methods have generated controversy with respect to the assumed topography of the callosal fibers [48]. In a previous study [7], we demonstrated that the pre-definition of callosal regions can give rise to erroneous results. To overcome these limits, some studies investigated callosal morphology using ROI analysis, which does not involve traditional parcellation [20,43,46], or applying an automated technique, such as VBM [8,10,20,66], which completely eliminates the manual tracing step.

Nevertheless, the VBM technique also has limitations. One limitation is related to the variety of options available for implementing the VBM [49,116]. Senjem et al. [49] found that 1) changes in the image processing chain of the VBM noticeably influenced the results of inter-group morphometric comparisons; and 2) optimized VBM, using custom template and prior images, improved the plausibility of inter-group comparisons, presumably due to improved segmentation and spatial normalization. Thus, optimized VBM produces different results from those obtained with standard VBM. Prior to Senjem et al. [49], other authors had already

pointed out the importance of spatial normalization, emphasizing that imperfect spatial normalization may affect the validity of VBM results [64,117,118].

There may be several reasons for the discrepant findings in DWI and DTI studies. First, the anisotropy indices from DWI are estimated from ADCs in three orthogonal directions, resulting in rotationally variant measurements that might differ if patients' heads have different sizes and are not oriented in the same way [119]. Thus, results are influenced by the different head positions of the subjects. DTI studies represent a step forward in this direction, because the scalar quantities associated with diffusion tensor (D) are invariant with respect to rotation of the coordinate system and, therefore, independent of the laboratory reference frame in which D is measured (i.e., they have the same value irrespective of the relative orientation of the "laboratory" and "fiber" frames of reference) [120]. Another aspect that can in part explain the variability in the results of DWI and DTI studies is how accurate the studies are in determining the location of changes. The latter can be inferred basically from ROI analyses [40,41,89], voxel-wise comparisons [32,82,84], or projecting diffusion values onto a tract-based template (TBSS) [85]. These approaches, however, all make assumptions about the correspondence of tract locations across subjects [121].

Moreover, with respect to the ROI analyses (the ones most frequently adopted in the DTI studies we reviewed; see Table 3), variability of results can be accounted for by the size and the placement of the ROIs across studies. As the placement of the ROIs is operator-dependent, care must be taken to place the ROIs only in WM areas to avoid partial volume effects through CSF spaces. This is because intravoxel fiber incoherence diminishes the measured FA value. Thus, large ROIs are more likely to include other tissue than just WM, diminishing the FA value. Furthermore, the number of ROIs simultaneously examined in the studies and the difference in sample size (fixed vs variable) can influence results.

Furthermore, the VBM-style approach in DTI studies presents problems related to image registration and smoothing [122]. The first aspect can be generally expressed as the confidence we have that any given standard space voxel contains data from the same part of the same WM tract in each subject. A second problem with VBM-style analyses is the standard practice of spatially smoothing data before computing voxel-wise statistics. In fact, the amount of smoothing can greatly affect the final results, but there is no princi-

pled way of deciding how much smoothing is the "correct" amount [123]. Smoothing also increases effective partial volume effect, a problem with VBM-style approaches particularly when applied to data such as FA. The use of TBSS [21,85,87] seems to overcome the limitations due to alignment of FA images from multiple subjects and to the arbitrariness of choosing the degree of spatial smoothing. TBSS solves these issues by means of carefully tuned nonlinear registration followed by projection onto an alignment-invariant tract representation (the "mean FA skeleton") with no spatial smoothing. This projection step removes the effect of cross-subject spatial variability that remains after the non-linear registration.

New possibilities in the research of WM callosal anatomy arise from the use of DTI in conjunction with fiber tractography. DTI-based tractography provides unique access to *in vivo* information about the topography of callosal fibers [48,124]. The technique allows reconstruction of the topographic arrangement of transcallosal fiber tracts projecting into specific cortical areas. Basically two ROIs are drawn, one is the entire CC and the other is each cortical area of projection. Then, a fiber tracking software is used to compute a 3D trajectory between the two ROIs. In both studies cited [48,124], the streamline fiber tracking method was based on fiber assignment by continuous tracking (FACT) [125]. The track trajectories follow the principal eigenvectors (the principal orientation of the fiber tract within the WM). When the 3D fiber track trajectory enters a neighboring voxel, the fiber track's direction is altered to match the direction of the new voxel's primary eigenvector. The 3D fiber track is allowed to continue from voxel to voxel until it enters a region of FA less than 0.02, turns an angle greater than 50° between two consecutive voxels, or exits the brain.

Thus, DTI-based tractography is able to give information about the anatomical parcellation and cortical connectivity of CC subregions. This aspect is of great interest especially for those neurodegenerative disorders that affect the transcallosal connectivity.

However, DTI-based tractography has its own limits: it is prone to noise, partial volume effects, crossing fibers and to image resolution. Thus, future works would substantially benefit from DTI-based tractography especially if the limits of the technique will be improved with a better spatial resolution of DTI acquisitions, a greater number of diffusion-encoding gradients, and a more adequate representation of orientational distributions.

Conclusions

Overall, the data suggest that studying the CC contributes to understanding the mechanisms underlying the progression of WM changes in AD and to expanding knowledge of its role in cerebral cognitive functioning. For this purpose, the application of different MRI techniques (e.g., traditional structural MRI and DTI) is crucial, because the measurement of multimodal parameters can offer a clearer picture of the WM in AD.

ACKNOWLEDGMENTS

We wish to thank Dr Roberta Querini for her precious help in finding the articles and Mr. Gregory Lynn Oxidine for his help in editing the manuscript. This work was in part supported by the Italian Ministry of Health (RF.06-07-08 and RC 06-07-08-09/A).

Authors' disclosures available online (<http://www.j-alz.com/disclosures/view.php?id=214>).

REFERENCES

- [1] Hua X, Leow AD, Parikshak N, Lee S, Chiang MC, Toga AW, Jack CR, Jr., Weiner MW, Thompson PM (2008) Tensor-based morphometry as a neuroimaging biomarker for Alzheimer's disease: an MRI study of 676 AD, MCI, and normal subjects. *Neuroimage* **43**, 458-469.
- [2] Hua X, Leow AD, Lee S, Klunder AD, Toga AW, Lepore N, Chou YY, Brun C, Chiang MC, Barysheva M, Jack CR, Jr., Bernstein MA, Britson PJ, Ward CP, Whitwell JL, Borowski B, Fleisher AS, Fox NC, Boyes RG, Barnes J, Harvey D, Kornak J, Schuff N, Boreta L, Alexander GE, Weiner MW, Thompson PM, Alzheimer's Disease Neuroimaging I (2008) 3D characterization of brain atrophy in Alzheimer's disease and mild cognitive impairment using tensor-based morphometry. *Neuroimage* **41**, 19-34.
- [3] Bronge L, Bogdanovic N, Wahlund LO (2002) Post-mortem MRI and histopathology of white matter changes in Alzheimer brains. A quantitative, comparative study. *Dement Geriatr Cogn Disord* **13**, 205-212.
- [4] Smith CD, Snowdon DA, Wang H, Markesbery WR (2000) White matter volumes and periventricular white matter hyperintensities in aging and dementia. *Neurology* **54**, 838-842.
- [5] Scheltens P, Barkhof F, Leys D, Wolters EC, Ravid R, Kamphorst W (1995) Histopathologic correlates of white matter changes on MRI in Alzheimer's disease and normal aging. *Neurology* **45**, 883-888.
- [6] Brun A, Englund E (1986) A white matter disorder in dementia of the Alzheimer type: a pathoanatomical study. *Ann Neurol* **19**, 253-262.
- [7] Tomaiuolo F, Scapin M, Di Paola M, Le Nezet P, Fadda L, Musicco M, Caltagirone C, Collins DL (2007) Gross anatomy of the corpus callosum in Alzheimer's disease: regions of degeneration and their neuropsychological correlates. *Dement Geriatr Cogn Disord* **23**, 96-103.
- [8] Chaim TM, Duran FL, Uchida RR, Perico CA, de Castro CC, Busatto GF (2007) Volumetric reduction of the corpus callosum in Alzheimer's disease *in vivo* as assessed with voxel-based morphometry. *Psychiatry Res* **154**, 59-68.
- [9] Wang PJ, Saykin AJ, Flashman LA, Wishart HA, Rabin LA, Santulli RB, McHugh TL, MacDonald JW, Mamourian AC (2006) Regionally specific atrophy of the corpus callosum in AD, MCI and cognitive complaints. *Neurobiol Aging* **27**, 1613-1617.
- [10] Thomann PA, Wustenberg T, Pantel J, Essig M, Schroder J (2006) Structural changes of the corpus callosum in mild cognitive impairment and Alzheimer's disease. *Dement Geriatr Cogn Disord* **21**, 215-220.
- [11] Teipel SJ, Bayer W, Alexander GE, Bokde AL, Zebuhr Y, Teichberg D, Muller-Spahn F, Schapiro MB, Moller HJ, Rapoport SI, Hampel H (2003) Regional pattern of hippocampus and corpus callosum atrophy in Alzheimer's disease in relation to dementia severity: evidence for early neocortical degeneration. *Neurobiol Aging* **24**, 85-94.
- [12] Teipel SJ, Bayer W, Alexander GE, Zebuhr Y, Teichberg D, Kulic L, Schapiro MB, Moller HJ, Rapoport SI, Hampel H (2002) Progression of corpus callosum atrophy in Alzheimer disease. *Arch Neurol* **59**, 243-248.
- [13] Hampel H, Teipel SJ, Alexander GE, Pogarell O, Rapoport SI, Moller HJ (2002) *In vivo* imaging of region and cell type specific neocortical neurodegeneration in Alzheimer's disease. Perspectives of MRI derived corpus callosum measurement for mapping disease progression and effects of therapy. Evidence from studies with MRI, EEG and PET. *J Neural Transm* **109**, 837-855.
- [14] Yamauchi H, Fukuyama H, Nagahama Y, Katsumi Y, Hayashi T, Oyanagi C, Konishi J, Shio H (2000) Comparison of the pattern of atrophy of the corpus callosum in frontotemporal dementia, progressive supranuclear palsy, and Alzheimer's disease. *J Neurol Neurosurg Psychiatry* **69**, 623-629.
- [15] Teipel SJ, Hampel H, Pietrini P, Alexander GE, Horwitz B, Daley E, Moller HJ, Schapiro MB, Rapoport SI (1999) Region-specific corpus callosum atrophy correlates with the regional pattern of cortical glucose metabolism in Alzheimer disease. *Arch Neurol* **56**, 467-473.
- [16] Thompson PM, Moussai J, Zohoori S, Goldkorn A, Khan AA, Mega MS, Small GW, Cummings JL, Toga AW (1998) Cortical variability and asymmetry in normal aging and Alzheimer's disease. *Cereb Cortex* **8**, 492-509.
- [17] Teipel SJ, Hampel H, Alexander GE, Schapiro MB, Horwitz B, Teichberg D, Daley E, Hippus H, Moller HJ, Rapoport SI (1998) Dissociation between corpus callosum atrophy and white matter pathology in Alzheimer's disease. *Neurology* **51**, 1381-1385.
- [18] Hampel H, Teipel SJ, Alexander GE, Horwitz B, Teichberg D, Schapiro MB, Rapoport SI (1998) Corpus callosum atrophy is a possible indicator of region- and cell type-specific neuronal degeneration in Alzheimer disease: a magnetic resonance imaging analysis. *Arch Neurol* **55**, 193-198.
- [19] Lyoo IK, Satlin A, Lee CK, Renshaw PF (1997) Regional atrophy of the corpus callosum in subjects with Alzheimer's disease and multi-infarct dementia. *Psychiatry Res* **74**, 63-72.
- [20] Di Paola M, Luders E, Di Iulio F, Varsi AE, Sancesario G, Passafiume D, Thompson PM, Caltagirone C, Toga AW, Spalletta G (2010) Callosal atrophy in mild cognitive impairment and Alzheimer's disease: Different effects in different stages. *Neuroimage* **49**, 141-149.
- [21] Di Paola M, Di Iulio F, Cherubini A, Blundo C, Casini AR, Sancesario G, Passafiume D, Caltagirone C, Spalletta G

- (2010b) When, where and how corpus callosal changes in preclinical and clinical AD using multimodal MRI at 3 Tesla. *Neurology*, in press.
- [22] Tomimoto H, Lin JX, Matsuo A, Ihara M, Ohtani R, Shibata M, Miki Y, Shibasaki H (2004) Different mechanisms of corpus callosum atrophy in Alzheimer's disease and vascular dementia. *J Neurol* **251**, 398-406.
- [23] Fellgiebel A, Wille P, Muller MJ, Winterer G, Scheurich A, Vucurevic G, Schmidt LG, Stoeter P (2004) Ultrastructural hippocampal and white matter alterations in mild cognitive impairment: a diffusion tensor imaging study. *Dement Geriatr Cogn Disord* **18**, 101-108.
- [24] Pantel J, Schroder J, Essig M, Minakaran R, Schad LR, Friedlinger M, Jauss M, Knopp MV (1998) Corpus callosum in Alzheimer's disease and vascular dementia – a quantitative magnetic resonance study. *J Neural Transm Suppl* **54**, 129-136.
- [25] Pantel J, Schroder J, Jauss M, Essig M, Minakaran R, Schonknecht P, Schneider G, Schad LR, Knopp MV (1999) Topography of callosal atrophy reflects distribution of regional cerebral volume reduction in Alzheimer's disease. *Psychiatry Res* **90**, 181-192.
- [26] Leys D, Pruvo JP, Parent M, Vermersch P, Soetaert G, Steiling M, Delacourte A, Defossez A, Rapoport A, Clarisse J, Petit H (1991) Could Wallerian degeneration contribute to leuko-araiosis in subjects free of any vascular disorder? *J Neurol Neurosurg Psychiatry* **54**, 46-50.
- [27] Kaufer DI, Miller BL, Itti L, Fairbanks LA, Li J, Fishman J, Kushi J, Cummings JL (1997) Midline cerebral morphometry distinguishes frontotemporal dementia and Alzheimer's disease. *Neurology* **48**, 978-985.
- [28] Hanyu H, Asano T, Sakurai H, Imon Y, Iwamoto T, Takasaki M, Shindo H, Abe K (1999) Diffusion-weighted and magnetization transfer imaging of the corpus callosum in Alzheimer's disease. *J Neurol Sci* **167**, 37-44.
- [29] Hanyu H, Imon Y, Sakurai H, Iwamoto T, Takasaki M, Shindo H, Kakizaki D, Abe K (1999) Regional differences in diffusion abnormality in cerebral white matter lesions in patients with vascular dementia of the Binswanger type and Alzheimer's disease. *Eur J Neurol* **6**, 195-203.
- [30] Sandson TA, Felician O, Edelman RR, Warach S (1999) Diffusion-weighted magnetic resonance imaging in Alzheimer's disease. *Dement Geriatr Cogn Disord* **10**, 166-171.
- [31] Black SE, Moffat SD, Yu DC, Parker J, Stanev P, Bronskill M (2000) Callosal atrophy correlates with temporal lobe volume and mental status in Alzheimer's disease. *Can J Neurol Sci* **27**, 204-209.
- [32] Rose SE, Chen F, Chalk JB, Zelaya FO, Strugnell WE, Benson M, Semple J, Doddrell DM (2000) Loss of connectivity in Alzheimer's disease: an evaluation of white matter tract integrity with colour coded MR diffusion tensor imaging. *J Neurol Neurosurg Psychiatry* **69**, 528-530.
- [33] Bozzao A, Floris R, Baviera ME, Apruzzese A, Simonetti G (2001) Diffusion and perfusion MR imaging in cases of Alzheimer's disease: correlations with cortical atrophy and lesion load. *AJNR Am J Neuroradiol* **22**, 1030-1036.
- [34] Good CD, Johnsrude IS, Ashburner J, Henson RN, Friston KJ, Frackowiak RS (2001) A voxel-based morphometric study of ageing in 465 normal adult human brains. *Neuroimage* **14**, 21-36.
- [35] Bozzali M, Falini A, Franceschi M, Cercignani M, Zuffi M, Scotti G, Comi G, Filippi M (2002) White matter damage in Alzheimer's disease assessed *in vivo* using diffusion tensor magnetic resonance imaging. *J Neurol Neurosurg Psychiatry* **72**, 742-746.
- [36] Takahashi S, Yonezawa H, Takahashi J, Kudo M, Inoue T, Tohgi H (2002) Selective reduction of diffusion anisotropy in white matter of Alzheimer disease brains measured by 3.0 Tesla magnetic resonance imaging. *Neurosci Lett* **332**, 45-48.
- [37] Head D, Buckner RL, Shimony JS, Williams LE, Akbudak E, Conturo TE, McAvoy M, Morris JC, Snyder AZ (2004) Differential vulnerability of anterior white matter in nondemented aging with minimal acceleration in dementia of the Alzheimer type: evidence from diffusion tensor imaging. *Cereb Cortex* **14**, 410-423.
- [38] Wiltshire K, Foster S, Kaye JA, Small BJ, Camicioli R (2005) Corpus callosum in neurodegenerative diseases: findings in Parkinson's disease. *Dement Geriatr Cogn Disord* **20**, 345-351.
- [39] Teipel SJ, Stahl R, Dietrich O, Schoenberg SO, Perneczky R, Bokde AL, Reiser MF, Moller HJ, Hampel H (2007) Multivariate network analysis of fiber tract integrity in Alzheimer's disease. *Neuroimage* **34**, 985-995.
- [40] Stahl R, Dietrich O, Teipel SJ, Hampel H, Reiser MF, Schoenberg SO (2007) White matter damage in Alzheimer disease and mild cognitive impairment: assessment with diffusion-tensor MR imaging and parallel imaging techniques. *Radiology* **243**, 483-492.
- [41] Zhang Y, Schuff N, Jahng GH, Bayne W, Mori S, Schad L, Mueller S, Du AT, Kramer JH, Yaffe K, Chui H, Jagust WJ, Miller BL, Weiner MW (2007) Diffusion tensor imaging of cingulum fibers in mild cognitive impairment and Alzheimer disease. *Neurology* **68**, 13-19.
- [42] Li S, Pu F, Shi F, Xie S, Wang Y, Jiang T (2008) Regional white matter decreases in Alzheimer's disease using optimized voxel-based morphometry. *Acta Radiol* **49**, 84-90.
- [43] Hallam BJ, Brown WS, Ross C, Buckwalter JG, Bigler ED, Tschanz JT, Norton MC, Welsh-Bohmer KA, Breitner JC (2008) Regional atrophy of the corpus callosum in dementia. *J Int Neuropsychol Soc* **14**, 414-423.
- [44] Witelson SF (1989) Hand and sex differences in the isthmus and genu of the human corpus callosum. A postmortem morphological study. *Brain* **112**(Pt 3), 799-835.
- [45] Hensel A, Wolf H, Kruggel F, Riedel-Heller SG, Nikolaus C, Arendt T, Gertz HJ (2002) Morphometry of the corpus callosum in patients with questionable and mild dementia. *J Neurol Neurosurg Psychiatry* **73**, 59-61.
- [46] Wang H, Su MY (2006) Regional pattern of increased water diffusivity in hippocampus and corpus callosum in mild cognitive impairment. *Dement Geriatr Cogn Disord* **22**, 223-229.
- [47] Weis S, Jellinger K, Wenger E (1991) Morphometry of the corpus callosum in normal aging and Alzheimer's disease. *J Neural Transm Suppl* **33**, 35-38.
- [48] Hofer S, Frahm J (2006) Topography of the human corpus callosum revisited – comprehensive fiber tractography using diffusion tensor magnetic resonance imaging. *Neuroimage* **32**, 989-994.
- [49] Senjem ML, Gunter JL, Shiung MM, Petersen RC, Jack CR, Jr. (2005) Comparison of different methodological implementations of voxel-based morphometry in neurodegenerative disease. *Neuroimage* **26**, 600-608.
- [50] Petersen RC, Smith GE, Waring SC, Ivnik RJ, Tangalos EG, Kokmen E (1999) Mild cognitive impairment: clinical characterization and outcome. *Arch Neurol* **56**, 303-308.
- [51] Petersen RC (2004) Mild cognitive impairment as a diagnostic entity. *J Intern Med* **256**, 183-194.

- [52] Lopez OL, Kuller LH, Becker JT, Dulberg C, Sweet RA, Gach HM, Dekosky ST (2007) Incidence of dementia in mild cognitive impairment in the cardiovascular health study cognition study. *Arch Neurol* **64**, 416-420.
- [53] Sydykova D, Stahl R, Dietrich O, Ewers M, Reiser MF, Schoenberg SO, Moller HJ, Hampel H, Teipel SJ (2007) Fiber connections between the cerebral cortex and the corpus callosum in Alzheimer's disease: a diffusion tensor imaging and voxel-based morphometry study. *Cereb Cortex* **17**, 2276-2282.
- [54] Jancke L, Staiger JF, Schlaug G, Huang Y, Steinmetz H (1997) The relationship between corpus callosum size and forebrain volume. *Cereb Cortex* **7**, 48-56.
- [55] Jancke L, Preis S, Steinmetz H (1999) The relation between forebrain volume and midsagittal size of the corpus callosum in children. *Neuroreport* **10**, 2981-2985.
- [56] Wang PP, Doherty S, Hesselink JR, Bellugi U (1992) Callosal morphology concurs with neurobehavioral and neuropathological findings in two neurodevelopmental disorders. *Arch Neurol* **49**, 407-411.
- [57] Schmitt JE, Eliez S, Warsofsky IS, Bellugi U, Reiss AL (2001) Corpus callosum morphology of Williams syndrome: relation to genetics and behavior. *Dev Med Child Neurol* **43**, 155-159.
- [58] Hensel A, Wolf H, Busse A, Arendt T, Gertz HJ (2005) Association between global brain volume and the rate of cognitive change in elderly humans without dementia. *Dement Geriatr Cogn Disord* **19**, 213-221.
- [59] Ortiz Alonso T, Martinez Castillo E, Fernandez Lucas A, Arrazola Garcia J, Maestu Unturbe F, Lopez-Ibor JJ (2000) Callosal atrophy and associated electromyographic responses in Alzheimer's disease and aging. *Electromyogr Clin Neurophysiol* **40**, 465-475.
- [60] Luders E, Narr KL, Zaidel E, Thompson PM, Jancke L, Toga AW (2006) Parasagittal asymmetries of the corpus callosum. *Cereb Cortex* **16**, 346-354.
- [61] Thompson PM, MacDonald D, Mega MS, Holmes CJ, Evans AC, Toga AW (1997) Detection and mapping of abnormal brain structure with a probabilistic atlas of cortical surfaces. *J Comput Assist Tomogr* **21**, 567-581.
- [62] Thompson PM, Schwartz C, Toga AW (1996) High-resolution random mesh algorithms for creating a probabilistic 3D surface atlas of the human brain. *Neuroimage* **3**, 19-34.
- [63] Thompson PM, Schwartz C, Lin RT, Khan AA, Toga AW (1996) Three-dimensional statistical analysis of sulcal variability in the human brain. *J Neurosci* **16**, 4261-4274.
- [64] Ashburner J, Friston KJ (2000) Voxel-based morphometry – the methods. *Neuroimage* **11**, 805-821.
- [65] Ashburner J, Friston KJ (2005) Unified segmentation. *Neuroimage* **26**, 839-851.
- [66] Good CD, Scahill RI, Fox NC, Ashburner J, Friston KJ, Chan D, Crum WR, Rossor MN, Frackowiak RS (2002) Automatic differentiation of anatomical patterns in the human brain: validation with studies of degenerative dementias. *Neuroimage* **17**, 29-46.
- [67] Basser PJ, Jones DK (2002) Diffusion-tensor MRI: theory, experimental design and data analysis – a technical review. *NMR Biomed* **15**, 456-467.
- [68] Neil J, Miller J, Mukherjee P, Huppi PS (2002) Diffusion tensor imaging of normal and injured developing human brain – a technical review. *NMR Biomed* **15**, 543-552.
- [69] Beaulieu C (2002) The basis of anisotropic water diffusion in the nervous system – a technical review. *NMR Biomed* **15**, 435-455.
- [70] Assaf BA, Mohamed FB, Abou-Khaled KJ, Williams JM, Yazeji MS, Haselgrove J, Faro SH (2003) Diffusion tensor imaging of the hippocampal formation in temporal lobe epilepsy. *AJNR Am J Neuroradiol* **24**, 1857-1862.
- [71] Sun SW, Song SK, Harms MP, Lin SJ, Holtzman DM, Merchant KM, Kotyk JJ (2005) Detection of age-dependent brain injury in a mouse model of brain amyloidosis associated with Alzheimer's disease using magnetic resonance diffusion tensor imaging. *Exp Neurol* **191**, 77-85.
- [72] Bartzokis G (2004) Age-related myelin breakdown: a developmental model of cognitive decline and Alzheimer's disease. *Neurobiol Aging* **25**, 5-18; author reply 49-62.
- [73] Song SK, Sun SW, Ju WK, Lin SJ, Cross AH, Neufeld AH (2003) Diffusion tensor imaging detects and differentiates axon and myelin degeneration in mouse optic nerve after retinal ischemia. *Neuroimage* **20**, 1714-1722.
- [74] Song SK, Sun SW, Ramsbottom MJ, Chang C, Russell J, Cross AH (2002) Dysmyelination revealed through MRI as increased radial (but unchanged axial) diffusion of water. *Neuroimage* **17**, 1429-1436.
- [75] Choi SJ, Lim KO, Monteiro I, Reisberg B (2005) Diffusion tensor imaging of frontal white matter microstructure in early Alzheimer's disease: a preliminary study. *J Geriatr Psychiatry Neurol* **18**, 12-19.
- [76] Muller MJ, Greverus D, Dellani PR, Weibrich C, Wille PR, Scheurich A, Stoeter P, Fellgiebel A (2005) Functional implications of hippocampal volume and diffusivity in mild cognitive impairment. *Neuroimage* **28**, 1033-1042.
- [77] Sundgren PC, Dong Q, Gomez-Hassan D, Mukherji SK, Maly P, Welsh R (2004) Diffusion tensor imaging of the brain: review of clinical applications. *Neuroradiology* **46**, 339-350.
- [78] Ray KM, Wang H, Chu Y, Chen YF, Bert A, Hasso AN, Su MY (2006) Mild cognitive impairment: apparent diffusion coefficient in regional gray matter and white matter structures. *Radiology* **241**, 197-205.
- [79] Naggara O, Oppenheim C, Rieu D, Raoux N, Rodrigo S, Dalla Barba G, Meder JF (2006) Diffusion tensor imaging in early Alzheimer's disease. *Psychiatry Res* **146**, 243-249.
- [80] Duan JH, Wang HQ, Xu J, Lin X, Chen SQ, Kang Z, Yao ZB (2006) White matter damage of patients with Alzheimer's disease correlated with the decreased cognitive function. *Surg Radiol Anat* **28**, 150-156.
- [81] Pierpaoli C, Basser PJ (1996) Toward a quantitative assessment of diffusion anisotropy. *Magn Reson Med* **36**, 893-906.
- [82] Xie S, Xiao JX, Gong GL, Zang YF, Wang YH, Wu HK, Jiang XX (2006) Voxel-based detection of white matter abnormalities in mild Alzheimer disease. *Neurology* **66**, 1845-1849.
- [83] Ukmar M, Makuc E, Onor ML, Garbin G, Trevisiol M, Cova MA (2008) Evaluation of white matter damage in patients with Alzheimer's disease and in patients with mild cognitive impairment by using diffusion tensor imaging. *Radiol Med* **113**, 915-922.
- [84] Medina D, DeToledo-Morrell L, Urresta F, Gabrieli JD, Moseley M, Fleischman D, Bennett DA, Leurgans S, Turner DA, Stebbins GT (2006) White matter changes in mild cognitive impairment and AD: A diffusion tensor imaging study. *Neurobiol Aging* **27**, 663-672.
- [85] Damoiseaux JS, Smith SM, Witter MP, Arigita EJ, Barkhof F, Scheltens P, Stam CJ, Zarei M, Rombouts SA (2009) White matter tract integrity in aging and Alzheimer's disease. *Hum Brain Mapp* **30**, 1051-1059.
- [86] Parente DB, Gasparetto EL, da Cruz LC, Jr., Domingues RC,

- Baptista AC, Carvalho AC, Domingues RC (2008) Potential role of diffusion tensor MRI in the differential diagnosis of mild cognitive impairment and Alzheimer's disease. *AJR Am J Roentgenol* **190**, 1369-1374.
- [87] Zarei M, Johansen-Berg H, Smith S, Ciccarelli O, Thompson AJ, Matthews PM (2006) Functional anatomy of interhemispheric cortical connections in the human brain. *J Anat* **209**, 311-320.
- [88] Rose SE, McMahon KL, Janke AL, O'Dowd B, de Zubicaray G, Strudwick MW, Chalk JB (2006) Diffusion indices on magnetic resonance imaging and neuropsychological performance in amnesic mild cognitive impairment. *J Neurol Neurosurg Psychiatry* **77**, 1122-1128.
- [89] Shim YS, Yoon B, Shon YM, Ahn KJ, Yang DW (2008) Difference of the hippocampal and white matter microalterations in MCI patients according to the severity of subcortical vascular changes: neuropsychological correlates of diffusion tensor imaging. *Clin Neurol Neurosurg* **110**, 552-561.
- [90] Cho H, Yang DW, Shon YM, Kim BS, Kim YI, Choi YB, Lee KS, Shim YS, Yoon B, Kim W, Ahn KJ (2008) Abnormal integrity of corticocortical tracts in mild cognitive impairment: a diffusion tensor imaging study. *J Korean Med Sci* **23**, 477-483.
- [91] Wang L, Goldstein FC, Veledar E, Levey AI, Lah JJ, Meltzer CC, Holder CA, Mao H (2009) Alterations in cortical thickness and white matter integrity in mild cognitive impairment measured by whole-brain cortical thickness mapping and diffusion tensor imaging. *AJNR Am J Neuroradiol* **30**, 893-899.
- [92] Zarei M, Damoiseaux JS, Morgese C, Beckmann CF, Smith SM, Matthews PM, Scheltens P, Rombouts SA, Barkhof F (2009) Regional white matter integrity differentiates between vascular dementia and Alzheimer disease. *Stroke* **40**, 773-779.
- [93] Braak H, Braak E (1997) Frequency of stages of Alzheimer-related lesions in different age categories. *Neurobiol Aging* **18**, 351-357.
- [94] Schmahmann JD PD (2006) *Fiber pathways of the brain*, Oxford University Press, New York.
- [95] Thompson PM, Hayashi KM, de Zubicaray G, Janke AL, Rose SE, Semple J, Herman D, Hong MS, Dittmer SS, Dordrell DM, Toga AW (2003) Dynamics of gray matter loss in Alzheimer's disease. *J Neurosci* **23**, 994-1005.
- [96] Braak H, Braak E (1991) Neuropathological staging of Alzheimer-related changes. *Acta Neuropathol* **82**, 239-259.
- [97] Galton CJ, Patterson K, Xuereb JH, Hodges JR (2000) Atypical and typical presentations of Alzheimer's disease: a clinical, neuropsychological, neuroimaging and pathological study of 13 cases. *Brain* **123**(Pt 3), 484-498.
- [98] Aboitiz F, Rodriguez E, Olivares R, Zaidel E (1996) Age-related changes in fibre composition of the human corpus callosum: sex differences. *Neuroreport* **7**, 1761-1764.
- [99] Aboitiz F, Scheibel AB, Fisher RS, Zaidel E (1992) Fiber composition of the human corpus callosum. *Brain Res* **598**, 143-153.
- [100] Petrides M (2005) Lateral prefrontal cortex: architectonic and functional organization. *Philos Trans R Soc Lond B Biol Sci* **360**, 781-795.
- [101] Petrides M (2002) The mid-ventrolateral prefrontal cortex and active mnemonic retrieval. *Neurobiol Learn Mem* **78**, 528-538.
- [102] Petrides M (1996) Specialized systems for the processing of mnemonic information within the primate frontal cortex. *Philos Trans R Soc Lond B Biol Sci* **351**, 1455-1461; discussion 1461-1452.
- [103] Brun A, Englund E (2002) Regional pattern of degeneration in Alzheimer's disease: neuronal loss and histopathological grading. *Histopathology* **41**, 40-55.
- [104] Brun A, Englund E (1981) Regional pattern of degeneration in Alzheimer's disease: neuronal loss and histopathological grading. *Histopathology* **5**, 549-564.
- [105] Bartzokis G, Cummings JL, Sultzer D, Henderson VW, Nuechterlein KH, Mintz J (2003) White matter structural integrity in healthy aging adults and patients with Alzheimer disease: a magnetic resonance imaging study. *Arch Neurol* **60**, 393-398.
- [106] Bartzokis G, Sultzer D, Lu PH, Nuechterlein KH, Mintz J, Cummings JL (2004) Heterogeneous age-related breakdown of white matter structural integrity: implications for cortical disconnection in aging and Alzheimer's disease. *Neurobiol Aging* **25**, 843-851.
- [107] Nieuwenhuys R (1999) Structure and organization of fibre systems In *The central nervous system of vertebrates.*, ed. S, ed., Berlin.
- [108] Tang Y, Nyengaard JR, Pakkenberg B, Gundersen HJ (1997) Age-induced white matter changes in the human brain: a stereological investigation. *Neurobiol Aging* **18**, 609-615.
- [109] Hildebrand C, Remahl S, Persson H, Bjartmar C (1993) Myelinated nerve fibres in the CNS. *Prog Neurobiol* **40**, 319-384.
- [110] Meier-Ruge W, Ulrich J, Bruhlmann M, Meier E (1992) Age-related white matter atrophy in the human brain. *Ann N Y Acad Sci* **673**, 260-269.
- [111] Levy R (1994) Aging-associated cognitive decline. Working Party of the International Psychogeriatric Association in collaboration with the World Health Organization. *Int Psychogeriatr* **6**, 63-68.
- [112] Richards M, Touchon J, Ledesert B, Richie K (1999) Cognitive decline in ageing: are AAMI and AACD distinct entities? *Int J Geriatr Psychiatry* **14**, 534-540.
- [113] Busse A, Bischkopf J, Riedel-Heller SG, Angermeyer MC (2003) Mild cognitive impairment: prevalence and incidence according to different diagnostic criteria. Results of the Leipzig Longitudinal Study of the Aged (LEILA75+). *Br J Psychiatry* **182**, 449-454.
- [114] Frisoni GB, Pievani M, Testa C, Sabatelli F, Bresciani L, Bonetti M, Beltramello A, Hayashi KM, Toga AW, Thompson PM (2007) The topography of grey matter involvement in early and late onset Alzheimer's disease. *Brain* **130**, 720-730.
- [115] Karas G, Scheltens P, Rombouts S, van Schijndel R, Klein M, Jones B, van der Flier W, Vrenken H, Barkhof F (2007) Precuneus atrophy in early-onset Alzheimer's disease: a morphometric structural MRI study. *Neuroradiology* **49**, 967-976.
- [116] Keller SS, Wilke M, Wiesmann UC, Sluming VA, Roberts N (2004) Comparison of standard and optimized voxel-based morphometry for analysis of brain changes associated with temporal lobe epilepsy. *Neuroimage* **23**, 860-868.
- [117] Bookstein FL (2001) Voxel-based morphometry should not be used with imperfectly registered images. *Neuroimage* **14**, 1454-1462.
- [118] Salmond CH, Ashburner J, Vargha-Khadem F, Connelly A, Gadian DG, Friston KJ (2002) The precision of anatomical normalization in the medial temporal lobe using spatial basis functions. *Neuroimage* **17**, 507-512.
- [119] Kantarci K, Jack CR, Jr., Xu YC, Campeau NG, O'Brien PC, Smith GE, Ivnik RJ, Boeve BF, Kokmen E, Tangalos EG, Petersen RC (2001) Mild cognitive impairment and Alzheimer

- disease: regional diffusivity of water. *Radiology* **219**, 101-107.
- [120] Basser PJ, Mattiello J, LeBihan D (1994) MR diffusion tensor spectroscopy and imaging. *Biophys J* **66**, 259-267.
- [121] Johansen-Berg H, Behrens TE (2006) Just pretty pictures? What diffusion tractography can add in clinical neuroscience. *Curr Opin Neurol* **19**, 379-385.
- [122] Smith SM, Jenkinson M, Johansen-Berg H, Rueckert D, Nichols TE, Mackay CE, Watkins KE, Ciccarelli O, Cader MZ, Matthews PM, Behrens TE (2006) Tract-based spatial statistics: voxelwise analysis of multi-subject diffusion data. *Neuroimage* **31**, 1487-1505.
- [123] Jones DK, Symms MR, Cercignani M, Howard RJ (2005) The effect of filter size on VBM analyses of DT-MRI data. *Neuroimage* **26**, 546-554.
- [124] Huang H, Zhang J, Jiang H, Wakana S, Poetscher L, Miller MI, van Zijl PC, Hillis AE, Wytik R, Mori S (2005) DTI tractography based parcellation of white matter: application to the mid-sagittal morphology of corpus callosum. *Neuroimage* **26**, 195-205.
- [125] Mori S, Crain BJ, Chacko VP, van Zijl PC (1999) Three-dimensional tracking of axonal projections in the brain by magnetic resonance imaging. *Ann Neurol* **45**, 265-269.
- [126] Kang YW, Na DL, Hahn SH (1997) A validity study on the Korean Mini-Mental State Examination (K-MMSE) in dementia patients. *J Korean Neurol Assoc* **15**, 300-308.
- [127] Duara R, Kushch A, Gross-Glenn K, Barker WW, Jallad B, Pascal S, Loewenstein DA, Sheldon J, Rabin M, Levin B, Lubs H (1991) Neuroanatomic differences between dyslexic and normal readers on magnetic resonance imaging scans. *Arch Neurol* **48**, 410-416.
- [128] Larsen JP, Höien T, Ödegaard H (1992) Magnetic resonance imaging of the corpus callosum in developmental dyslexia. *Cogn Neuropsychol* **9**, 123-134.